POLITECNICO DI MILANO

Scuola di Ingegneria Industriale e dell'Informazione
Laurea Magistrale in Ingegneria Matematica

Poisson-Maxwell-Stefan modeling of mass transport in electronics applications

Relatore: **Prof. Riccardo Sacco**
Correlatore: **Dr. Aurelio Giancarlo Mauri**

Daniele Carlo Corti
Matr. 852637

Anno Accademico 2017-2018

Contents

List of Figures

List of Tables

Sommario

Questo elaborato di tesi si concentra sulla modellazione matematica del fenomeno fisico del trasporto di massa nelle miscele, applicata alle memorie a cambiamento di fase (Phase Change Memory, PCM). Fra i modelli matematici sviluppati per questo fine, il modello di Maxwell-Stefan coniuga due aspetti fondamentali: da un lato, fornisce tutti gli strumenti necessari per una analisi esauriente del movimento delle specie chimiche nelle miscele diluite e non diluite; dall'altro consente di includere nelle equazioni, con relativa facilità, tutte le generiche forze che possono agire su un sistema fisico.

A causa dell'accoppiamento e della non-linearità delle equazioni che lo compongono, la risoluzione di questo modello richiede l'utilizzo di tecniche di iterazione funzionale quali il metodo di Newton e la mappa di Gummel. La discretizzazione delle equazioni è stata effettuata con il metodo di Galerkin agli elementi finiti.

Sono stati svolti numerosi test, nel caso di miscele diluite i risultati ottenuti sono stati confrontati con quelli forniti da modelli validati in letteratura, ad esempio il modello di Fick per la diffusione e il modello di Poisson-Nernst-Planck. Questi modelli possono essere interpretati come casi limite per miscele diluite del più generale modello di Maxwell-Stefan.

Abstract

This thesis focuses on the mathematical modeling of the physical phenomenon of mass transport in mixtures, applied to phase change memories (Phase Change Memory, PCM). Among the mathematical models developed for this purpose, the Maxwell-Stefan model combines two fundamental aspects: on one hand, it provides all the tools necessary for an exaustive analysis of the movement of chemical species in diluted and undiluted mixtures; on the other hand, it allows us to include in the equations, quite easily, all the generic forces that can act on a physical system.

Because of the coupling and non-linearity of the equations, the resolution of this model requires the use of functional iteration techniques such as the Newton method and the Gummel Map. The discretization of the equations was performed with the Galerkin Finite Element Method.

Numerous tests have been carried out, in the case of diluted mixtures the results obtained have been compared with those provided by models validated in the literature, for example the Fick model of diffusion and the Poisson-Nernst-Planck model. These models can be interpreted as limit cases for dilute mixtures of the more general Maxwell-Stefan model.

Introduction

The need of reliable high-performance memory devices has led in recent years several microelectronics and semiconductor companies to develop a new generation of electronics memories, the so-called Phase Change Memories(PCM). This kind of memories exploits the properties of chalcogenide materials to change their phase from the amorphous phase to the crystalline phase. During the phase change, sufficiently high temperatures are reached to cause mass transport inside these devices which may compromise the correct operation of the device. In order to improve the reliability of these devices it is therefore essential to be able to analyze and understand the mass transport phenomenon. For this purpose, the Maxwell-Stefan model is introduced and analyzed.

This document is structured as follows:

Chapter 1 introduction to the mode of operation of a PCM and an overview of the main physical phenomena to be included in the model with regard to mass transport;

Chapter 2 presentation of the Maxwell-Stefan model starting from the analysis of the interactions between chemical species up to the equations in their most general form. Comparison between the Maxwell-Stefan model and the Fick model of diffusion;

Chapter 3 inclusion of the electric field and the thermal field in the Maxwell-Stefan equations, introduction of the Poisson equation for the electric potential. Formulation of an iterative algorithm for the solution of the Poisson-Maxwell-Stefan model;

Chapter 4 weak formulation of the equations and analysis of a good position of each step of the iterative algorithm;

Chapter 5 discretization of the equations and solution through the Galerkin Finite Element Method and details on the implementation of the code;

Chapter 6 tests on the Maxwell-Stefan model and comparison with Fick diffusion models. Comparison between Poisson-Maxwell-Stefan and Poisson-Nernst-Planck models.

Chapter 1

Introduction to Phase Change Memories

Phase Change Memories(PCM) constitute one of the most promising example of nanotechnology in advanced non-volatile solid state devices for data writing, reading and storage. Offering excellent performances, good scalability and high reliability, this device represents the state of the art of memory production.

This type of memories exploit the great difference in resistivity between the crystalline and the amorphous phase of phase change materials. Chalcogenide materials in amorphous phase (Figure 1.1a) have a high resistivity, while in the cristaline phase (Figure 1.1b) they have a low resistivity.

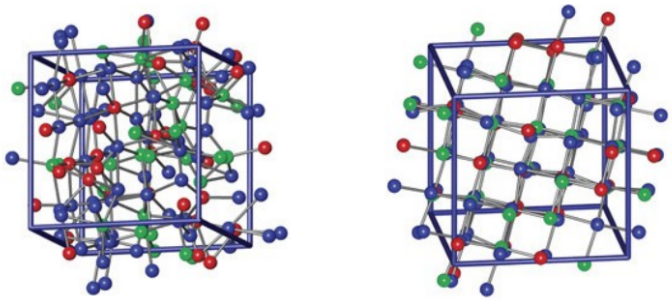

(a) Amorphous phase (b) Cristaline phase

Figure 1.1: Comparison between the disordered amorphous phase (a) and the ordered cristaline phase (b)

To set the PCM cell to an amorphous state, a large current pulse is applied which, by Joule effect, melts the affected region; the latter, quickly quenched, remains in an amorphous state (see Figure 1.2). On the other hand, to set the PCM cell on a crystalline phase, a medium current impulse is applied which brings the region concerned to a temperature lower than the melting temperature but higher than the crystallization temperature for a sufficiently long interval time, typically between 100 $ns - 1\mu s$, to crystallize.

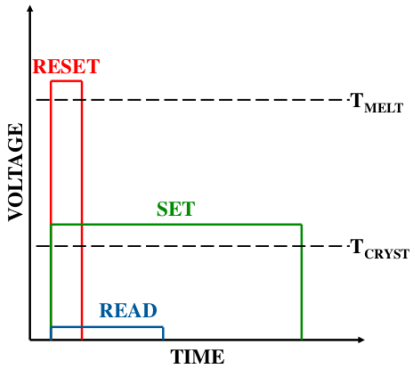

Figure 1.2: Qualitative time-voltage relation for the phase change

One of the most used materials in these applications is the $Ge_2Sb_2Te_5$, an alloy of Germanium, Antimony and Tellurium, which offers a good compromise between electrical properties and phase change velocity. This alloy is also known as GST-225.

Modeling PCM devices, from a physical and mathematical point of view, represents a complex challenge due to the multitude of phenomena to be considered: drift, diffusion, thermal effects, state and phase transitions, etc.

In particular, these devices, for the whole duration of their life, are subjected to high electrical and thermal stresses that cause the movement of the atoms that make up the alloy. Phenomena of this kind, which occur above all near the melting point where the mobility of atoms are higher, create variations in the composition of the material both in space and in time. These variations have important consequences on the performance and reliability of the device.

For a complete description of the device as a whole, we need a model

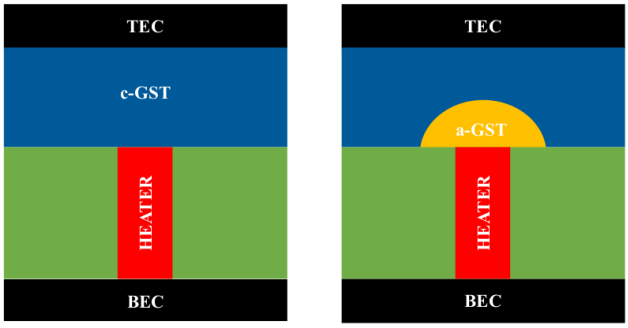

Figure 1.3: Cross section of a PCM cell, c-GST and a-GST regions correspond to region in the crystalline or the amorphous phase, respectively

that takes into account all the above mentioned physical phenomena that are created and therefore includes: the Poisson equation for the electrical potential, the heat equation for the temperature, a model for phase change, for drift-diffusion and eventually for mass transport.

One of the most used models for mass transport is the following [15]:

$$\begin{cases} \dfrac{\partial c}{\partial t} + \nabla \cdot \boldsymbol{N} = 0 & \text{(1.1a)} \\ \boldsymbol{N}_i = -D\left(\nabla c + \dfrac{z^* q}{k_b T} c \nabla \varphi + \alpha c \dfrac{\nabla T}{T}\right) & \text{(1.1b)} \end{cases}$$

where c is the concentration, D is the phase and temperature dependent diffusivity and z^* is the effective charge. Essentially, the considered model is an extension of the Fick model for diffusion, which is represented by the first term in (1.1b). The second term considers the effect of the electric field while the third term considers the effect of temperature. The electrical potential and temperature functions are given respectively by the Poisson and heat equation. The equation system (1.1) is solved using the finite element method for each of the chemical species that constitute the alloy, three considering the GST-225, to which are added an equal number of suitable initial conditions.

Experimental evidence shows a significant deviation of the experimental data from the predictions of the mathematical model (1.1). In order to provide a more accurate description of mass transport, accounting also for

the effects of the electric field and temperature, we propose in the present thesis the Maxwell-Stefan model. In the following chapters, we illustrate the physical background of the formulation, we provide theoretical results of its well-posedness and a computational algorithm for its approximate solution. Simulation results are also discussed in detail for a validation of proposed model and methods.

Chapter 2

The Maxwell-Stefan Model

In this chapter we introduce the *Maxwell-Stefan* model for mass transport in gaseous and liquid mixtures [11][12]. With this aim, we start from the analysis of the interaction between the chemical species that constitute the mixture and then we consider the most general forces that can act on the physical system. We conclude the presentation with a comparison between the Maxwell-Stefan model and the Fick model.

2.1 Introduction and notation

Mass transport is the transfer of mass or, on a microscopic scale, the movement of atoms or molecules of a given material or substance due to the action of different drivers, such as temperature and electric field.

In the applications of our interest in the present work, materials and substances are usually *mixtures*. Mixtures are a combination of chemical species such that each species retains its own chemical identity and chemical bonds between the species are neither broken nor formed. In particular, a *binary mixture* is composed by two chemical species, whereas a *multicomponent mixture* is composed by two or more chemical species. If the concentration of a species, let us say the nth one, is much larger than the concentration of all the other species, the mixture is called *diluted*. The nth species is named *solvent* and the others are named *solutes*. In a dilute mixture, all the interactions between solutes can be considered negligible. Diluted or undiluted mixtures that have thermodynamic properties analogous to those of a mixtures of ideal gases are named *ideal mixtures*.

Let us introduce the definitions of some physical quantities that will be useful for the development and comprehension of Maxwell-Stefan's theory:

Name	Description	unit of measure
n	number of species in the mixture	$[-]$
c_i	molar density of species i	$\left[mol\ m^{-3}\right]$
ρ_i	density of species i	$\left[kg\ m^{-3}\right]$
n_i	number density of species i	$\left[m^{-3}\right]$
c_t	total molar density	$\left[mol\ m^{-3}\right]$
ρ_t	total density	$\left[kg\ m^{-3}\right]$
n_t	total number density	$\left[m^{-3}\right]$
x_i	molar fraction of species i	$[-]$
ω_i	mass fraction of species i	$[-]$
$\boldsymbol{u}_i$	velocity of species i	$\left[m\ s^{-1}\right]$
$\boldsymbol{u}$	average velocity	$\left[m\ s^{-1}\right]$
$\boldsymbol{N}_i$	molar flux of species i	$\left[mol\ m^{-2}\ s^{-1}\right]$
$\boldsymbol{N}_t$	total molar flux	$\left[mol\ m^{-2}\ s^{-1}\right]$
$\boldsymbol{J}_i$	relative molar flux of species i	$\left[mol\ m^{-2}\ s^{-1}\right]$
μ_i	molar chemical potential of species i	$\left[J\ mol^{-1}\right]$

Table 2.1: Useful physical quantities

The following relations among the variables are assumed to hold:

$$c_t = \sum_{i=1}^{n} c_i \tag{2.1a}$$

$$c_i = x_i c_t \quad \longrightarrow \quad 0 \leq x_i \leq 1 \tag{2.1b}$$

$$\boldsymbol{u} = \sum_{i=1}^{n} x_i \boldsymbol{u}_i \tag{2.1c}$$

$$\boldsymbol{N}_i = c_i \boldsymbol{u}_i \tag{2.1d}$$

$$\boldsymbol{N}_t = \sum_{i=1}^{n} \boldsymbol{N}_i = \sum_{i=1}^{n} c_t x_i \boldsymbol{u}_i = c_t \boldsymbol{u} \tag{2.1e}$$

$$\boldsymbol{J}_i = c_i \left(\boldsymbol{u}_i - \boldsymbol{u}\right) = \boldsymbol{N}_i - c_i \boldsymbol{u} \tag{2.1f}$$

$$\sum_{i=1}^{n} \boldsymbol{J}_i = \boldsymbol{0} \tag{2.1g}$$

Using equations (2.1b) and (2.1a) we obtain the following constraint for the molar fractions

$$\sum_{i=1}^{n} x_i = 1 \tag{2.2}$$

The transport regime corresponding to the condition $\boldsymbol{N}_t = \boldsymbol{0}$, is called *equimolar diffusion*. In this case, (2.1e) implies that:

$$\boldsymbol{u} = \boldsymbol{0} \tag{2.3a}$$

$$\boldsymbol{N}_t = \sum_{i=1}^{n} \boldsymbol{N}_i = \boldsymbol{0} \tag{2.3b}$$

Let us consider a chemical species i; the number density n_i and the total number density n_t are related to the molar densities c_i and c_t through the relations:

$$n_i = N_A c_i \tag{2.4a}$$

$$n_t = N_A c_t \tag{2.4b}$$

whereas the density ρ_i and the total density ρ_t are related to the molar densities c_i and c_t through the relations:

$$\rho_i = M_i c_i \tag{2.5a}$$

$$\rho_t = \sum_{i=1}^{n} \rho_i = c_t \sum_{i=1}^{n} x_i M_i \tag{2.5b}$$

$$\omega_i = \frac{\rho_i}{\rho_t} \tag{2.5c}$$

where N_A is the *Avogadro constant* $\left[6.022e23\ mol^{-1}\right]$ and M_i is the molar mass of species i $(kg\ mol^{-1})$.

2.2 Duncan and Toor experiment

Before analyzing thoroughly the Maxwell-Stefan relations, we illustrate in this section an experiment conducted by *Duncan and Toor* in 1962 [3] since it shows important feature that can not be explained by the standard Fick's law of diffusion.

The experiment set-up consists in two bulb cells connectet by a capillary tube. At time $t = 0$ the molar fractions of the three gases which constitute the ideal mixture are:

	Hydrogen	Nitrogen	Carbon dioxide
Bulb 1	$x_1 = 0.00000$	$x_2 = 0.50086$	$x_3 = 0.49914$
Bulb 2	$x_1 = 0.50121$	$x_2 = 0.49879$	$x_3 = 0.00000$

In addition, the pressure and the temperature are constant in space and time. We remark that during the experiment there is equimolar diffusion of the species, that means no net transfer of flux out of or into the system.
For the hydrogen and the nitrogen molar fractions experiment results are reported in Figure 2.1, whereas the molar fraction of the carbon dioxide can be deduced by recalling that they all sum up to one.

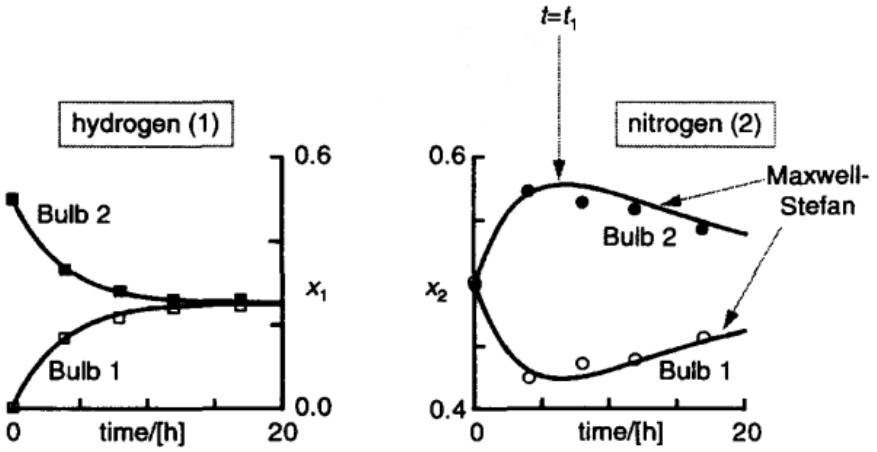

(a) Hydrogen (b) Nitrogen

Figure 2.1: Results of Duncan-Toor experiment

In Figure 2.1 the squares and dots represent experimental data, white for bulb 1 and black for bulb 2. The solid lines are the predictions of the Maxwell-Stefan model.

Examining the two graphs in Figure 2.1 we find that the time trajectory of the hydrogen molar follows the classic *Fick's* diffusion moldel, mathematically represented by formula (2.6), whereas the nitrogen molar fraction does not follow the classic Fick law.

$$\boldsymbol{J}_i = c_i \left(\boldsymbol{u}_i - \boldsymbol{u}\right) = -c_t D_i \nabla x_i \qquad D_i > 0 \quad i = 1, \ldots, n \tag{2.6}$$

As can be seen from the graph in Figure 2.1b, the temporal trajectories

of the nitrogen show four different phenomena defined by *Toor* in [22] and called:

Osmotic diffusion : flux in absence of molar fraction gradient ($\nabla x_2 \approx 0$), shown at $t = 0$;

Reverse diffusion : flux in opposite direction of the molar fraction gradient $\left(\frac{\boldsymbol{J}_2}{-\nabla x_2} < 0\right)$, shown in $0 < t < t_1$;

Diffusion barrier : null flux despite a big molar fraction gradient, at $t = t_1$:

Standard diffusion : flux direction and the molar fraction gradient direction agree, from $t > t_1$.

As a matter of fact *Fick's law* holds under the hypothesis of binary mixture or to describe the diffusion of a dilute species i in a multicomponent dilute mixture. It seems obvious that if, as in the Duncan and Toor experiment, undiluted species are treated, a more general model of diffusion is needed. An alternative formulation is the *Maxwell-Stefan* model that is described in Section 2.3.

2.3 Derivation of the Maxwell-Stefan relation

In this section we start with a two-component system, whereas we consider a more general setting in the next sections.

2.3.1 Diffusion in binary mixtures

In this section we want to explain the origins of the Maxwell-Stefan equations, thus we can start by taking as physical example the Duncan and Toor experiment. We consider a pipe through which atoms or molecules of two species, called 1 and 2, flow. By Newton's second law, the sum of the forces acting on a system is proportional to the rate of change of the momentum of the whole system, so we proceed by analyzing forces and momentum.

Considering the infinitesimal control volume represented in Figure 2.2, the forces acting on the volume can be body forces, such as gravity or electrical force, and surface forces, like pressure or shear stress. For simplicity we start by considering only the pressure exerted on the two faces of the

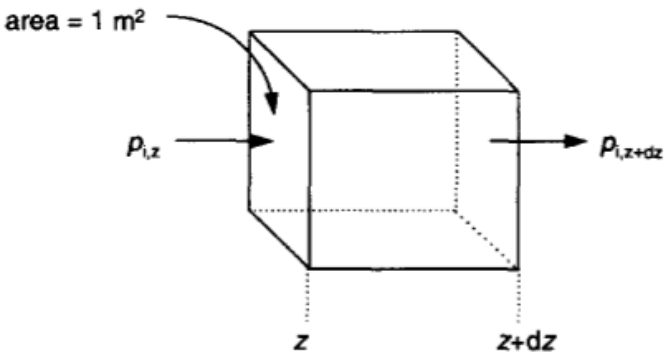

Figure 2.2: Control volume

control volume, normal to the z-direction.
Let P be the pressure exerted by the molecules outside the box and p_i be the partial pressure of the species i such that

$$p_i = Px_i$$

The force exerted by the molecules of type i on the left face is $\boldsymbol{T}_{i,z} = S\ p_{i,z}$ and the force exerted on the right face is $\boldsymbol{T}_{i,z+dz} = -S\ p_{i,z+dz}$. Therefore, the total force applied in the z-direction by species i is

$$\boldsymbol{T}_{tot,i,z} = \boldsymbol{T}_{i,z} + \boldsymbol{T}_{i,z+dz} = S(p_{i,z} - p_{i,z+dz}) \tag{2.7}$$

Dividing equation (2.7) by the volume $V = Sdz$ and passing to the limit for $dz \longrightarrow 0$ we obtain the force density $F_{i,z}$ of the species i in the z-direction.

$$\boldsymbol{F}_{tot,i,z} = -\frac{\partial p_i}{\partial z} \tag{2.8}$$

Considering the other two components of the force vector, the total force per unit of volume acting for each species i is

$$\boldsymbol{F}_{tot,i} = -\nabla p_i \qquad i = 1, 2 \tag{2.9}$$

Let us now investigate the mechanism of the collisions, that are assumed to be elastic, between two atomic or molecular species. We can consider an average molecule (i.e. an ideal molecule that represents the average of all the molecules) of species 1 and an average molecule of species 2, that

have momentum $m_1\boldsymbol{u}_1$ and $m_2\boldsymbol{u}_2$, respectively. When the two molecules collide the total momentum of the pair of molecules, that is $m_1\boldsymbol{u}_1 + m_2\boldsymbol{u}_2$, is conserved. Thus, introducing the velocities $\boldsymbol{u}_1^{'}$ and $\boldsymbol{u}_2^{'}$ of species 1 and 2 after collision, we have that

$$m_1\boldsymbol{u}_1 + m_2\boldsymbol{u}_2 = m_1\boldsymbol{u}_1^{'} + m_2\boldsymbol{u}_2^{'}$$

so we obtain the average velocity after collision of the species 1 that is [16]

$$\boldsymbol{u}_1^{'} = \frac{m_1\boldsymbol{u}_1 + m_2\boldsymbol{u}_2}{m_1 + m_2}$$

So the momentum that a molecule of species 1 transfers to a molecule of species 2 throught a collision is

$$\Delta M_1 = m_1\left(\boldsymbol{u}_1 - \boldsymbol{u}_1^{'}\right) = \frac{m_1 m_2\left(\boldsymbol{u}_1 - \boldsymbol{u}_2\right)}{m_1 + m_2}$$

The rate of change of momentum of species 1 per unit of volume is equal to the average momentum transferred by a collision multiplied by the number of collisions between 1 and 2 ($\propto x_1 x_2$) per unit of volume and time, that is

$$\frac{\partial M_1}{\partial t} \propto x_1 x_2\left(\boldsymbol{u}_1 - \boldsymbol{u}_2\right) \tag{2.10}$$

Combining (2.9) and (2.10) and introducing the proportionality coefficient $f_{1,2}$, we get

$$\nabla p_i = -f_{i,j} x_i x_j\left(\boldsymbol{u}_i - \boldsymbol{u}_j\right)$$

where $f_{1,2}$ must have the units $\left(kg\ m^{-3}s^{-1}\right)$. Defining the inverse drag coefficient $Đ_{1,2} = {}^{P}/_{f_{1,2}}\ (m^2 s^{-1})$ we can rewrite the previous equations as

$$\boldsymbol{d}_i = -\frac{\nabla p_i}{P} = \frac{x_i x_j\left(\boldsymbol{u}_i - \boldsymbol{u}_j\right)}{Đ_{ij}}$$

where $\boldsymbol{d}_i$ is the driving force of the species i in an ideal mixture at constant pressure and temperature. Thus $\boldsymbol{d}_i = {}^{\nabla p_i}/_{P} = \nabla x_i$ and the above equation becomes

$$\boldsymbol{d}_i = -\nabla x_i = \frac{x_i x_j\left(\boldsymbol{u}_i - \boldsymbol{u}_j\right)}{Đ_{ij}} \tag{2.11}$$

If we consider the case of a non ideal mixture, a chemical potential gradient arises in the thermodynamics of irreversible processes as the fundamental driving force for diffusion, therefore

$$\boldsymbol{d}_i = -\frac{x_i}{RT}\nabla_{T,P}\mu_i = \frac{x_i x_j\left(\boldsymbol{u}_i - \boldsymbol{u}_j\right)}{Đ_{ij}} \tag{2.12}$$

where $\nabla_{T,P}$ denotes the gradient at constant temperature and pressure. Equations (2.11) and (2.12) are the Maxwell-Stefan relations, respectively, for ideal and non-ideal binary mixtures at constant temperature and pressure.

Let γ_i be activity coefficient function of species i. Then, the chemical molar potential μ_i is defined as:

$$\mu_i := \mu_{i,0}(T,P) + RT \ln\left(\gamma_i \frac{p_i}{P}\right) = \mu_{i,0}(T,P) + RT \ln\left(\gamma_i x_i\right) \tag{2.13}$$

In particular, since the activity coefficient is used to account for deviations from ideal behavior, in ideal gases $\gamma_i = 1$.

2.3.2 Diffusion in a multicomponent mixture

In Section 2.3.1 we have obtained the Maxwell-Stefan equations for ideal or non-ideal binary solutions at constant temperature and pressure. The next step is to write the Maxwell-Stefan equations for a multicomponent mixture. In this case the interactions between the species are still supposed to be binary. In other words it is supposed that during the friction process the momentum transferred by species i to species j is independent of the presence of other species. Thus the momentum exchanged by species i is given by the sum of the momenta exchanged by the species i to all others. Mathematically we can say that the *superposition priciple* holds, and the Maxwell-Stefan equations for an ideal multicomponent mixture are

$$-\nabla x_i = \sum_{\substack{j=1 \\ j\neq i}}^{n} \frac{x_i x_j \left(\boldsymbol{u}_i - \boldsymbol{u}_j\right)}{Đ_{ij}} \qquad i = 1, \ldots, n \tag{2.14}$$

whereas in the case of a non-ideal multicomponent mixture we have

$$-\frac{x_i}{RT} \nabla_{T,P} \mu_i = \sum_{\substack{j=1 \\ j\neq i}}^{n} \frac{x_i x_j \left(\boldsymbol{u}_i - \boldsymbol{u}_j\right)}{Đ_{ij}} \qquad i = 1, \ldots, n \tag{2.15}$$

Equations (2.14) and (2.15) are the generalizations in the case of multicomponet mixtures of (2.11) and (2.12), respectively.

Starting from (2.15) and using the definition of chemical potential (2.13) it is possible to deduce the following relation for a multicomponent mixture

$$
\begin{aligned}
-\boldsymbol{d}_i &= \frac{x_i}{RT}\nabla_{T,P}\mu_i \\
&= \frac{x_i}{RT}\sum_{j=1}^{n-1}\left.\frac{\partial\mu_i}{\partial x_j}\right|_{T,P,\Sigma}\nabla x_j \\
&= x_i\sum_{j=1}^{n-1}\left(\frac{\partial \ln x_i}{\partial x_j} + \left.\frac{\partial \ln \gamma_i}{\partial x_j}\right|_{T,P,\Sigma}\right)\nabla x_j \\
&= \sum_{j=1}^{n-1}\left(\delta_{ij} + x_i\left.\frac{\partial \ln \gamma_i}{\partial x_j}\right|_{T,P,\Sigma}\right)\nabla x_j \\
&= \sum_{j=1}^{n-1}\Gamma_{ij}\nabla x_j
\end{aligned}
\tag{2.16}
$$

where

$$
\Gamma_{ij} = \delta_{ij} + x_i\left.\frac{\partial \ln \gamma_i}{\partial x_j}\right|_{T,P,\Sigma} \tag{2.17}
$$

In equation (2.16), δ_{ij} is the *Kronecker delta* and the subscript Σ means that the differentiation with respect to x_j must be evaluated considering constant all the other molar fractions except the nth one, because molar fractions sum up to one. For an ideal mixture $\gamma_i = 1$, thus relation (2.16) becomes

$$
\boldsymbol{d}_i = -\frac{x_i}{RT}\nabla_{T,P}\mu_i = -\nabla x_i \tag{2.18}
$$

that corresponds to (2.11) and (2.14).
Equation (2.15) can be also related to the fluxes $\boldsymbol{N}_i$ and $\boldsymbol{J}_i$ as follows

$$
\begin{aligned}
-\frac{x_i}{RT}\nabla_{T,P}\mu_i &= \sum_{\substack{j=1\\ j\neq i}}^{n}\frac{x_i x_j\left(\boldsymbol{u}_i - \boldsymbol{u}_j\right)}{Đ_{ij}} \\
&= \sum_{\substack{j=1\\ j\neq i}}^{n}\frac{x_j\boldsymbol{N}_i - x_i\boldsymbol{N}_j}{c_t\, Đ_{ij}} \qquad (2.19) \\
&= \sum_{\substack{j=1\\ j\neq i}}^{n}\frac{x_j\boldsymbol{J}_i + \cancel{x_j x_i\boldsymbol{N}_t} - x_i\boldsymbol{J}_j - \cancel{x_i x_j\boldsymbol{N}_t}}{c_t\, Đ_{ij}} \\
&= \sum_{\substack{j=1\\ j\neq i}}^{n}\frac{x_j\boldsymbol{J}_i - x_i\boldsymbol{J}_j}{c_t\, Đ_{ij}} \qquad (2.20)
\end{aligned}
$$

In a thermodynamical system the *Gibbs-Duhem* equation can be derived starting from the Gibbs free energy $\boldsymbol{G}$. The total differential of $\boldsymbol{G}$ in terms of its natural variables is

$$d\boldsymbol{G} = \left.\frac{\partial \boldsymbol{G}}{\partial p}\right|_{T,C} dp + \left.\frac{\partial \boldsymbol{G}}{\partial T}\right|_{p,C} dT + \sum_{i=1}^{n} \left.\frac{\partial \boldsymbol{G}}{\partial C_i}\right|_{p,T,C_{j\neq i}} dC_i$$

where C_i is the number of mole of component i, S the entropy, V the volume, T the temperature and p the pressure. Since the Gibbs free energy is the Legendre transformation of the internal energy, the derivatives can be replaced by its definitions transforming the above equation into:

$$d\boldsymbol{G} = V dp - S dT + \sum_{i=1}^{n} \mu_i dC_i \tag{2.21}$$

The chemical potential is simply another name for the partial molar Gibbs free energy. Thus it can be defined as

$$\boldsymbol{G} = \sum_{i=1}^{n} \mu_i C_i$$

and its total differential reads

$$d\boldsymbol{G} = \sum_{i=1}^{n} \mu_i dC_i + \sum_{i=1}^{n} C_i d\mu_i \tag{2.22}$$

Combining (2.21) and (2.22) we get

$$\sum_{i=1}^{n} \mu_i dC_i + \sum_{i=1}^{n} C_i d\mu_i = V dp - S dT + \sum_{i=1}^{n} \mu_i dC_i$$

which simplifies to the Gibbs-Duhem relation

$$\sum_{i=1}^{n} C_i d\mu_i = -S dT + V dp \tag{2.23}$$

Summing equation (2.15) on i we have

$$-\sum_{i=1}^{n} c_i \nabla_{T,P} \mu_i = R\, T \sum_{i=1}^{n} \sum_{\substack{j=1 \\ j\neq i}}^{n} \frac{x_j \boldsymbol{N}_i - x_i \boldsymbol{N}_j}{Đ_{ij}}$$

Dividing (2.23) by V and remembering that T and p are constant we obtain

$$-R\,T\sum_{i=1}^{n}\sum_{\substack{j=1\\ j\neq i}}^{n}\frac{x_j\boldsymbol{N}_i - x_i\boldsymbol{N}_j}{Đ_{ij}} = -\frac{S}{V}\nabla T + \nabla p = \mathbf{0} \tag{2.24}$$

The above relation shows that only $n-1$ of the n Maxwell-Stefan relations are linearly independent. Moreover this result shows that the Maxwell-Stefan approch is consistent with thermodynamics laws.

Remark: The constraints deriving from equation (2.23) are still valid even removing the assumption of constant pressure and temperature. Therefore, also in general cases, only $n-1$ Maxwell-Stefan relations are linearly independent.

2.4 Generalized driving force

In Section 2.3, we introduced the Maxwell-Stefan equations considering as a driving force only the gradient of the chemical potential at constant temperature and pressure. In this section, we analyze the Maxwell-Stefan relations considering generalized driving forces and we also remove the assumption of constant pressure while the temperature is still assumed constant.

Let $\boldsymbol{F}_i$ denote, a general molar body force acting per mole of species i. Then the generalized driving force $\boldsymbol{d}_i$ reads

$$\boldsymbol{d}_i = -\frac{x_i}{RT}\left(\nabla_T\mu_i - \boldsymbol{F}_i\right) \tag{2.25}$$

where ∇_T denotes the gradient at constant temperature. Let V_i be the partial molar volume of species i ($m^3\ mol^{-1}$), following relation holds

$$\nabla_T\mu_i = \nabla_{T,P}\mu_i + V_i\nabla P \tag{2.26}$$

Linear momentum balance implies

$$\frac{d\boldsymbol{v}}{dt} + \nabla\cdot\boldsymbol{\tau} = -\frac{1}{\rho_t}\nabla P + \sum_{i=1}^{n}\omega_i\tilde{\boldsymbol{F}}_i \tag{2.27}$$

where $\boldsymbol{v}$ is the mass average velocity ($m\ s^{-1}$), $\boldsymbol{\tau}$ is the stress tensor ($N\ m\ kg^{-1}$), $\tilde{\boldsymbol{F}}_i$ is the body force acting per kg of species i ($N\ kg^{-1}$) and the other variables are defined in Table 2.1.

In the hypothesis that mechanical equilibrium is reached faster than thermodynamical equilibrium we can suppose that

$$\frac{d\boldsymbol{v}}{dt} + \nabla \cdot \boldsymbol{\tau} \approx 0 = -\frac{1}{\rho_t}\nabla P + \sum_{i=1}^{n} \omega_i \tilde{\boldsymbol{F}}_i \tag{2.28}$$

Thus, multiplying the right hand side of (2.28) by the molar weight ρ_i/c_i of the species i we get

$$\begin{aligned} 0 &= \frac{1}{c_i}\left(-\frac{\rho_i}{\rho_t}\nabla P + \rho_i \sum_{j=1}^{n} \omega_j \tilde{\boldsymbol{F}}_j\right) \\ &= \frac{1}{c_i}\left(-\omega_i \nabla P + \frac{\rho_i}{\rho_t} \sum_{j=1}^{n} \rho_j \tilde{\boldsymbol{F}}_j\right) \\ &= \frac{1}{c_i}\left(-\omega_i \nabla P + \omega_i \sum_{j=1}^{n} c_j \boldsymbol{F}_j\right) \end{aligned} \tag{2.29}$$

Adding (2.29) into (2.25) and using (2.26), equation (2.25) becomes

$$\begin{aligned} \boldsymbol{d}_i &= -\frac{x_i}{RT}\left(\nabla_{T,P}\mu_i + V_i \nabla P - \frac{\omega_i}{c_i}\nabla P + \frac{\omega_i}{c_i}\sum_{j=1}^{n} c_j \boldsymbol{F}_j - \boldsymbol{F}_i\right) \\ &= -\frac{x_i}{RT}\nabla_{T,P}\mu_i - \frac{(c_i V_i - \omega_i)}{c_t RT}\nabla P + \frac{1}{c_t RT}\left(c_i \boldsymbol{F}_i - \omega_i \sum_{j=1}^{n} c_j \boldsymbol{F}_j\right) \end{aligned} \tag{2.30}$$

Relation (2.30) is the expression of the generalized driving force for a non-ideal multicomponent mixture. Let us consider the case of an idel mixture for which the *ideal gas law* holds. We have that

$$PV_t = n_t RT \qquad c_t = \frac{n_t}{V_t} \tag{2.31}$$

where V_t is the mixture molar volume ($m^3\ mol^{-1}$). Using equation (2.31) into (2.30) we obtain

$$\boldsymbol{d}_i = -\nabla x_i - \frac{1}{P}\left(c_i V_i - \omega_i\right)\nabla P + \frac{1}{P}\left(c_i \boldsymbol{F}_i - \omega_i \sum_{j=1}^{n} c_j \boldsymbol{F}_j\right) \tag{2.32}$$

2.5 Thermal diffusion

In the case of electronics applications the temperature is no longer constant in space an time. Thus, we need to include it into the treatment of Section 2.3.2.

To do that we include in the Maxwell-Stefan model the *Soret effect* or *thermophoresis*, also known as *thermomigration* or *thermodiffusion*, which introduces a flux production due to temperature gradient. Thus, taking in account this phenomenon, equation (2.15) becomes

$$\boldsymbol{d}_i = -\sum_{\substack{j=1 \\ j\neq i}}^{n} \frac{x_i x_j \left(\boldsymbol{u}_i - \boldsymbol{u}_j\right)}{Đ_{ij}} - \sum_{\substack{j=1 \\ j\neq i}}^{n} \frac{x_i x_j}{Đ_{ij}} \left(\frac{D_i^T}{\rho_i} - \frac{D_j^T}{\rho_j}\right) \frac{\nabla T}{T} \tag{2.33}$$

where D_i^T $(kg\ m^{-1}\ s^{-1})$ is the thermal diffusion coefficient of species i. Equation (2.33) can be more conveniently written as

$$\boldsymbol{d}_i = -\sum_{\substack{j=1 \\ j\neq i}}^{n} \frac{x_i x_j \left(\boldsymbol{u}_i^T - \boldsymbol{u}_j^T\right)}{Đ_{ij}} \tag{2.34}$$

where $\boldsymbol{u}_i^t$ is the velocity $(m\ s^{-1})$ of the species i that includes the thermal diffusion contribution

$$\boldsymbol{u}_i^T = \boldsymbol{u}_i + \left(\frac{\boldsymbol{D}_i^T}{\rho_i}\right) \frac{\nabla T}{T} = \boldsymbol{u}_i + \alpha_i \frac{\nabla T}{T}$$

where α_i $(m^2\ s^{-1})$, named thermal diffusivity of the species i, is given by

$$\alpha_i = \frac{D_i^T}{\rho_i} \tag{2.35}$$

2.6 General Maxwell-Stefan relation

In the previous sections we have initially introduced the Maxwell-Stefan relations for binary mixtures, then we have extended them to multicomponent mixtures and we have considered general driving forces, and, finally, we have added thermal effects. Now, combining equations (2.30) and (2.34), we are

in a position to write the *general Maxwell-Stefan relations*

$$-\frac{x_i}{RT}\nabla_{T,p}\mu_i - \frac{1}{c_t RT}\left(c_i V_i - \omega_i\right)\nabla p + \frac{1}{c_t RT}\left(c_i \boldsymbol{F}_i - \omega_i \sum_{j=1}^{n} c_j \boldsymbol{F}_j\right) = \sum_{\substack{j=1 \\ j\neq i}}^{n} \frac{x_i x_j \left(\boldsymbol{u}_i^T - \boldsymbol{u}_j^T\right)}{Đ_{ij}} \tag{2.36}$$

Using the second law of thermodynamics the following results can be proven (see [6]).

$$Đ_{ij} = Đ_{ji} \tag{2.37}$$

$$Đ_{ij} > 0 \qquad \text{for an ideal mixture} \tag{2.38}$$

2.7 A comparison between Maxwell-Stefan and Fick model of diffusion

In this section we are interested to understand the relation (if any) between Maxwell-Stefan and Fick model of diffusion. For simplicity, we consider only the driving force provided by the molar fractions, neglecting other external forces. Thus relation (2.15), using (2.20) and (2.16), becomes

$$\sum_{\substack{j=1 \\ j\neq i}}^{n} \frac{x_j \boldsymbol{J}_i - x_i \boldsymbol{J}_j}{c_t\, Đ_{ij}} = -\sum_{j=1}^{n-1} \Gamma_{ij} \nabla x_i \qquad i = 1, \ldots, n$$

which can be written in matrix form as

$$\boldsymbol{B}\boldsymbol{J} = -c_t \boldsymbol{\Gamma} \nabla \boldsymbol{x}$$

where matrix $\boldsymbol{B}$ is defined as

$$B_{ii} = \frac{x_i}{Đ_{in}} + \sum_{\substack{j=1 \\ j\neq i}}^{n} \frac{x_j}{Đ_{ij}} \tag{2.39a}$$

$$B_{ij} = \left(\frac{1}{Đ_{in}} - \frac{1}{Đ_{ij}}\right) x_i \qquad i \neq j \tag{2.39b}$$

Based on the above result, equation (2.6) can be generalized as

$$\boldsymbol{J} = -c_t \boldsymbol{D} \nabla \boldsymbol{x} \tag{2.40}$$

that is called *generalized Fick law*, where

$$\boldsymbol{D} = \boldsymbol{B}^{-1} \boldsymbol{\Gamma} \tag{2.41}$$

Equation (2.40) shows that the Maxwell-Stefan model and the generalized Fick model of diffusion are mathematically equivalent. However, Maxwell-Stefan's approach is, in some respects, more convenient than the generalized Fick model. The $Đ_{ij}$ coefficients are independent of the composition of the mixture, whereas the Fick coefficients are not because of equation (2.41); moreover the coefficients $Đ_{ij}$ are also independent of the driving forces. Finally, the Maxwell-Stefan model can be easily extended to other driving forces. Unfortunately, the N_i flux is a function not only of the molar fractions $x_{j=1,\dots,n}$ but also of the other fluxes $N_{j\neq i}$, this leads to considerable difficulties in the solution of the numerical Maxwell-Stefan model.

Chapter 3

The Poisson-Maxwell-Stefan Model

The main aim of this thesis is to develop a mathematical model that describes the spatial and temporal evolution of the concentration profiles of the chemical species that constitute an undiluted mixture subject to an electric potential and a thermal field. In the present chapter we will use Maxwell-Stefan's relations (2.36) as the main ingredient for the construction of the above mentioned mathematical model.

3.1 Electric potential

3.1.1 Maxwell-Stefan relations for electric potential

To apply the Maxwell-Stefan model discussed in Chapter 2 in the context of electronics applications let us consider as a volumetric force the Electric field produced by the application of an external bias to an electronic device. Let φ be a given function denoting the electric potential and let $\boldsymbol{E} = -\nabla\varphi$ be the associated electric field. The force $\boldsymbol{F}_i$ produced by the electric field on the i-th species of the mixture is equal to

$$\boldsymbol{F}_i = z_i \mathcal{F} \boldsymbol{E} \tag{3.1}$$

where $\mathcal{F}$ is *Faraday's constant*$(96500\ C\ mol^{-1})$ and z_i is the electric charge number of the chemical species i. Note that only ionized species ($z_i \neq 0$) are directly affected by the presence of an external electric field.

Assuming the action of a given thermal effect and electric field, equations (2.36) become

$$\begin{aligned}\sum_{\substack{j=1\\j\neq i}}^{n}\frac{x_j\boldsymbol{N}_i - x_i\boldsymbol{N}_j}{c_t\text{Đ}_{ij}} + \sum_{\substack{j=1\\j\neq i}}^{n}\frac{x_i x_j\left(\alpha_i-\alpha_j\right)}{\text{Đ}_{ij}}\frac{\nabla T}{T}\\ = -\frac{x_i}{RT}\nabla_{T,p}\mu_i - \frac{x_i}{RT}\left(z_i - \omega_i\sum_{j=1}^{n}\frac{z_j x_j}{x_i}\right)\mathcal{F}\ \nabla\varphi\end{aligned} \tag{3.2}$$

It is convenient define the effective electric charge number (see Section 6.1.3) as

$$z_{i,eff} = \left(z_i - \omega_i\sum_{j=1}^{n}\frac{z_j x_j}{x_i}\right) \tag{3.3}$$

so equation (3.2) becomes

$$\begin{aligned}\sum_{\substack{j=1\\j\neq i}}^{n}\frac{x_j\boldsymbol{N}_i - x_i\boldsymbol{N}_j}{c_t\text{Đ}_{ij}} + \sum_{\substack{j=1\\j\neq i}}^{n}\frac{x_i x_j\left(\alpha_i-\alpha_j\right)}{\text{Đ}_{ij}}\frac{\nabla T}{T}\\ = -\frac{x_i}{RT}\nabla_{T,p}\mu_i - \frac{x_i}{RT}z_{i,eff}\mathcal{F}\ \nabla\varphi\end{aligned} \tag{3.4}$$

Assuming that the electroneutral condition holds in any points on the mixture (in this case the mixture is said electroneutral)

$$\sum_{j=1}^{n} z_j x_j = 0 \tag{3.5}$$

we have that $z_{i,eff} = z_i$ otherwise the $z_{i,eff}$ can be either greater or lower, with the same sign or not with respect to the ions charge number.

3.1.2 Poisson equation

The electric potential is a function of the external applied bias and of the spatial distribution of the electric charges, consequently it depends directly on the distribution of the chemical species composing the mixture. Since the concentrations of the species are also functions of time, we deduce that the electric potential will also have an indirect dependence on the time coordinate. To clarify this issue, let us start from the *Maxwell equations*, the

fundamental laws that govern electromagnetic interaction, [8]:

$$\nabla \times \boldsymbol{H} = \boldsymbol{J} + \frac{\partial \boldsymbol{D}}{\partial t} \tag{3.6a}$$

$$\nabla \times \boldsymbol{E} = -\frac{\partial \boldsymbol{B}}{\partial t} \tag{3.6b}$$

$$\nabla \cdot \boldsymbol{D} = \rho \tag{3.6c}$$

$$\nabla \cdot \boldsymbol{B} = 0 \tag{3.6d}$$

and the related constitutive equations, with absolute (or dielectric) permittivity ε and magnetic permeability μ_h, that characterize the properties of the medium:

$$\boldsymbol{D} = \varepsilon \boldsymbol{E} \tag{3.7a}$$

$$\boldsymbol{B} = \mu_m \boldsymbol{H} \tag{3.7b}$$

Using (3.6) and (3.7), we obtain an equation for the electric potential as follows. Because of the vector calculus identity $\nabla \cdot \nabla \times \boldsymbol{A} = 0$, equation (3.6d) is satisfied $\forall \boldsymbol{A}$ such that $\boldsymbol{B} = \nabla \times \boldsymbol{A}$. Replacing this relation in (3.6b) we get

$$\nabla \times \left(\boldsymbol{E} + \frac{\partial \boldsymbol{A}}{\partial t} \right) = 0$$

This latter relation implies that $\boldsymbol{E} + \frac{\partial \boldsymbol{A}}{\partial t}$ is irrotational and it follows that there exists a potential φ such that

$$\boldsymbol{E} + \frac{\partial \boldsymbol{A}}{\partial t} = -\nabla \varphi$$

Introducing the quasi-static approximation $\frac{\partial \boldsymbol{A}}{\partial t} = 0$ we obtain

$$\boldsymbol{E} = -\nabla \varphi \tag{3.8}$$

Combining (3.8), (3.7a) and (3.6c) we have the *Poisson equation*

$$-\nabla \cdot (\varepsilon \nabla \varphi) = \rho$$

The charge density ρ can be splitted into two parts: the fixed charge density and the mobile charge density.
The fixed charge density is obtained by multiplying the number density of the fixed charge P by the electron charge q. The mobile charge density is given by the sum on all the species of the products of the i-th species number density n_i, of the effective electric charge number z_i and of the electron charge q, so that the final form of the Poisson equation reads

$$-\nabla \cdot (\varepsilon \nabla \varphi) = q \left(\sum_{i=1}^{n} z_i n_i + P \right) \tag{3.9}$$

3.2 Poisson-Maxwell-Stefan model

The $n-1$ Maxwell-Stefan relations and the Poisson equation (3.9) introduce into the mathematical model n unknowns for the flows $\boldsymbol{N}_i$, n unknowns for the molar concentrations c_i and an unknown for the electric potential φ. The temperature T is assumed to be a given function on all the domain for each time instant. The variables n_i, x_i and c_t can be expressed as functions of c_i through the relations (2.1a), (2.1b) and (2.4a). Overall there are $2n+1$ unknowns but only $n-1$ equations, therefore we introduce n homogeneous continuity equations

$$\frac{\partial c_i}{\partial t} + \nabla \cdot \boldsymbol{N}_i = 0 \tag{3.10}$$

The right-hand side of (3.10) is equal to zero because net production effects due to mutual ion interaction can be safely neglected. The last two equations necessary for closing the system are provided by equation (2.2) and by the equimolar constraint (2.3), that is

$$\boldsymbol{N}_t = 0$$

The continuity equation of the total molar density

$$\frac{\partial c_t}{\partial t} + \nabla \cdot \boldsymbol{N}_t = 0 \tag{3.11}$$

is a linear combination of the continuity equations (3.10). Replacing the continuity equation of the species n with (3.11) and imposing the equimolar constraint we get that

$$\frac{\partial c_t}{\partial t} = 0 \longrightarrow c_t = c_t\left(\boldsymbol{x}\right)$$

but, because the initial molar concentrations $c_1^0, \ldots, c_n^0$ are known, we get

$$c_t(\boldsymbol{x}) = \sum_{i=1}^{n} c_i^0(\boldsymbol{x})$$

Thus the molar concentration of the species n can be computed by post-processing as

$$c_n = c_t - \sum_{i=1}^{n-1} c_i$$

so that only $n-1$ continuity equation are needed.

For simplicity, the subsequent analysis is limited to the case of ideal mixtures. Then equation (3.4) becomes:

$$\begin{aligned}\sum_{\substack{j=1\\j\neq i}}^{n}\frac{x_j\boldsymbol{N}_i-x_i\boldsymbol{N}_j}{c_t\text{Đ}_{ij}}+\sum_{\substack{j=1\\j\neq i}}^{n}\frac{x_ix_j\left(\alpha_i-\alpha_j\right)}{\text{Đ}_{ij}}\frac{\nabla T}{T}\\ =-\nabla x_i-\frac{x_i}{RT}z_{i,eff}\mathcal{F}\ \nabla\varphi\end{aligned}\tag{3.12}$$

Combining equations (3.12), (3.9) and (3.10) we end up with:

Model 1 (Poisson-Maxwell-Stefan)
Let Ω be a bounded domain of $\mathbb{R}^d$, d=1,2,3, $Q_T=\Omega\times(0,T)$, and $S_T=\partial\Omega\times(0,T)$, $T>0$, the Poisson-Maxwell-Stefan *model is given by*

$$\begin{cases}
c_t\dfrac{\partial x_i}{\partial t}+\nabla\cdot\boldsymbol{N}_i=0 & \text{in } Q_T \quad (3.13a)\\
\displaystyle\sum_{\substack{j=1\\j\neq i}}^{n}\frac{x_j\boldsymbol{N}_i-x_i\boldsymbol{N}_j}{c_t\text{Đ}_{ij}}+\sum_{\substack{j=1\\j\neq i}}^{n}\frac{x_ix_j\left(\alpha_i-\alpha_j\right)}{\text{Đ}_{ij}}\frac{\nabla T}{T}\\
\qquad=-\nabla x_i-\dfrac{x_i}{RT}z_{i,eff}\mathcal{F}\ \nabla\varphi & \text{in } Q_T \quad (3.13b)\\
z_{i,eff}=\left(z_i-\omega_i\displaystyle\sum_{j=1}^{n}\frac{z_jx_j}{x_i}\right) & (3.13c)\\
\displaystyle\sum_{i=1}^{n}x_i=1 & (3.13d)\\
\displaystyle\sum_{i=1}^{n}\boldsymbol{N}_i=0 & (3.13e)\\
-\nabla\cdot(\varepsilon\nabla\varphi)=q\left(\displaystyle\sum_{i=1}^{n}z_in_i+P\right) & \text{in } Q_T \quad (3.13f)\\
c_i(\boldsymbol{x},0)=\bar{c}_i(\boldsymbol{x}) & \text{in } \Omega \quad (3.13g)\\
\varphi=\bar{\varphi}_d & \text{on } S_T \quad (3.13h)\\
\boldsymbol{N}_i\cdot\nu=0 & \text{on } S_T \quad (3.13i)
\end{cases}$$

for every $i=1,\dots,n-1$.

The homogeneous Neumann boundary conditions (3.13i) for the fluxes are chosen as a consequence of the assumption of equimolar diffusion and of the fact that the physical system is closed. The interest on imposing an external electric potential difference justifies the choice of the non homogeneous Dirichlet boundary condition (3.13h).

The mathematical analysis and numerical sulution of the Poisson-Maxwell-Stefan model (3.13) is a non trivial task because:

1. the Maxwell-Stefan relations are strongly coupled, both for the molar fractions x_i and for the fluxes $\boldsymbol{N_i}$;
2. in addition, the total molar fraction c_t, the effective electric charge number $z_{i,eff}$ and the density fraction ω_i hide further non-linearity;
3. the Poisson equation, due to the dependence of the number density n_i, through the molar concentration, is coupled with the other equations.

To overcome the difficulties related to the nonlinear and coupled nature of system (3.13), suitable functional iterations must be used to compute an approximate solution.

3.3 Time step

The solution of a system of time dependent equations, such as (3.13), typically proceeds through the partition of the time domain $(0, T)$ into N_t temporal intervals,

$$\Delta t_i = t_i - t_{i-1} \qquad \forall i = 1, \dots, N_t$$

and then through the discretization of time derivatives using the Θ-method (cf. Section 5.2), and finally solving the time semidiscretized equations at each discrete time level. If the time intervals are uniform, i.e. $\Delta t_i = \Delta t_j \ \forall i, j = 1, \dots, N_t$, they are indicated with Δt.

The time advancing procedure (see Figure 3.1) can be summarized as follows

i) Given the initial molar concentration of the n chemical species $c_1^0, \dots, c_n^0$, the potential at initial time φ^0 can be computed by solving the Poisson equation (3.9) and by computing the initial fluxes $\boldsymbol{N}_1^0, \dots, \boldsymbol{N}_n^0$ through Maxwell-Stefan relations (3.12);

ii) through a decoupling loop solve the equations (3.13a), (3.13b) and (3.13f) to get φ^t and $c_1^t, \ldots, c_n^t$ at time level t ;

iii) compute fluxes $\boldsymbol{N}_1^t, \ldots, \boldsymbol{N}_n^t$ at time level t ;

iv) if time level $t < N_t$ get back to point ii), else (3.13) has been solved at each time level.

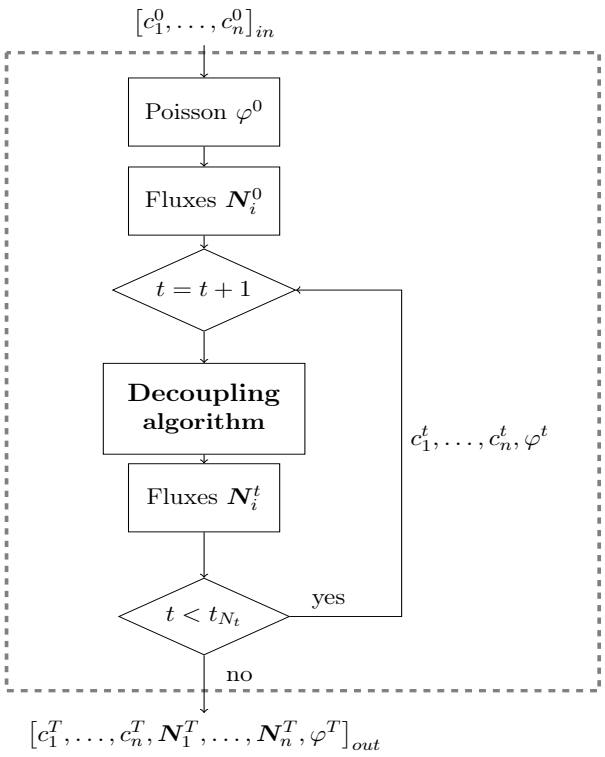

Figure 3.1: Time advancing scheme

3.4 Iterative algorithms

After having semi-discretized in time system (3.13) with one of the methods presented in Section 5.2, we and up with the following abstract nonlinear problem

$$\boldsymbol{F}(\boldsymbol{U}) = \boldsymbol{0} \tag{3.14}$$

where

$$\boldsymbol{U} := \left[\varphi, x_1, \ldots, x_n\right]^T \qquad \boldsymbol{F}\left(\boldsymbol{U}\right) := \begin{bmatrix} F_1\left(\boldsymbol{U}\right) \\ F_2\left(\boldsymbol{U}\right) \\ \vdots \\ F_{n-1}\left(\boldsymbol{U}\right) \end{bmatrix} \tag{3.15}$$

having set:

$$\begin{aligned} F_1\left(\boldsymbol{U}\right) &= -\nabla \cdot \left(\varepsilon \nabla \varphi\right) - q\left(\sum_{i=1}^{n} z_i n_i + P\right) \\ F_2\left(\boldsymbol{U}\right) &= \frac{c_1}{\Delta t} - \frac{c_1^{old}}{\Delta t} + \nabla \cdot \boldsymbol{N}_1 \\ \vdots & \quad \vdots \\ F_{n-1}\left(\boldsymbol{U}\right) &= \frac{c_{n-1}}{\Delta t} - \frac{c_{n-1}^{old}}{\Delta t} + \nabla \cdot \boldsymbol{N}_{n-1} \end{aligned}$$

In the above representation we have used the Backward Euler method for the time discretization and obtained $\boldsymbol{N}_1, \ldots, \boldsymbol{N}_{n-1}$ by relations (3.12). The problem we have to solve now is: given a functional space V and an operator $F : V \to V$, find $\boldsymbol{U} \in V$ such that (3.14) is satisfied. The most used iterative algorithms to solve system (3.14) are the *decoupled Gummel map* and the *fully coupled Newton's method*.

3.4.1 Gummel Map

The Gummel Map was proposed for the first time in 1964 by H. K. Gummel at the Bell Labs for the iterative solution of the Poisson-Drift-Diffusion problem [5]. Despite having a linear convergence rate, it presents some characteristics that make it more advisable to solve (3.14) than the Fully Coupled Newton Method:

- it is less sensitive to the choice of the initial guess;
- it has a lower computational cost;
- experimentally it shows a superlinear convergence rate.

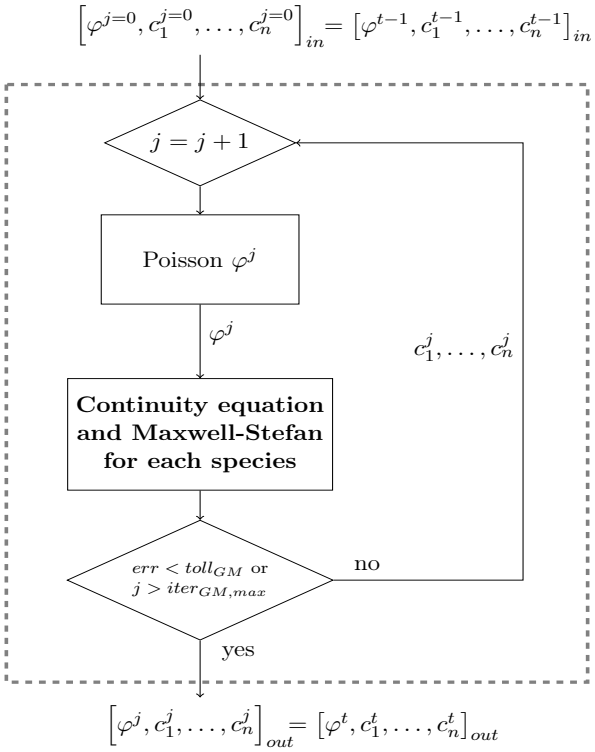

Figure 3.2: Gummel map scheme

An adaptation of Gummel's map to the solution of problem (3.13) is graphically represented in Figure 3.2(which corresponds to the "Decoupling algorithm" boxe in Figure 3.1), and can be divided into the following steps:

i) fix an initial guess φ^0, $c_1^0, \ldots, c_n^0$, a tolerance $toll_{GM} > 0$ and a maximum number of iterations $iter_{GM,max}$;

ii) solve the Poisson equation using Newton's method (see Section 3.4.2);

iii) solve the $n - 1$ continuity equations (3.13a) and the Maxwell-Stefan relations (3.13b);

iv) if the error between two consecutive iterations is less than $toll_{GM}$ or the number of iterations is larger than $iter_{GM,max}$, then the loop exits, otherwise we start from step (ii).

The full theoretical analysis of the convergence of Gummel's Map can be found in [9].

3.4.2 Newton's method

Definition 1 (Fréchet differentiability)
Let X and Y be Banach spaces, and $U \subseteq X$ a open subset of X. Let $\|\cdot\|_X$ and $\|\cdot\|_Y$ be the norm of space X and Y, respectively. A function operator $F : U \subseteq X \to Y$ is called Fréchet differentiable at $x_0 \in U$ if there exist an operator $L \in \mathcal{L}(X, Y)$ such that if $h \in U$ and $x_0 + h \in U$,

$$\lim_{\|h\| \to 0} \frac{\|F(x_0 + h) - F(x_0) - L(x_0)\, h\|_Y}{\|h\|_X} = 0 \tag{3.16}$$

$L(x_0)$ is called the Fréchet derivative of F at x_0 and we write $L(x_0) = F'(x_0)$.

The Newton method is defined as follow:

Definition 2 (Newton's method)
Let X and Y be Banach spaces and $F : X \to Y$ a function operator Frechèt differentiable, given an initial datum $\boldsymbol{U}^0 \in X$ and toll > 0, for all $k \geq 0$ solve the following linear problem:

$$\boldsymbol{F}'\left(\boldsymbol{U}^k\right) \delta \boldsymbol{U}^k = -\boldsymbol{F}\left(\boldsymbol{U}^k\right) \tag{3.17}$$

$$\boldsymbol{U}^{k+1} = \boldsymbol{U}^k + \delta \boldsymbol{U}^k \tag{3.18}$$

until $\left\|\boldsymbol{F}\left(\boldsymbol{U}^{k+1}\right)\right\|_Y < toll$.

The application of Newton's method has transformed the original problem (3.14), with $F : V \to V$, into the *fixed-point problem* of finding $U \in V$ such that

$$\boldsymbol{U} = T_{\boldsymbol{F}}(\boldsymbol{U})$$

where

$$T_{\boldsymbol{F}}(\boldsymbol{U}) = \boldsymbol{F}'(\boldsymbol{U})^{-1}\left(\boldsymbol{F}'(\boldsymbol{U})\,\boldsymbol{U} - \boldsymbol{F}(\boldsymbol{U})\right)$$

is the iteration function associated with the Newton method.

Definition 3 (Continuos linear operator)
Let X and Y be normed spaces. Then $L(X, Y)$ denotes the space of the continuous linear operator from X to Y. Moreover $L(X, Y)$ is a normed space with respect to the norm:

$$\|l\|_{L(X,Y)} := \sup_{\substack{x \in X \\ x \neq 0}} \frac{\|l(x)\|_Y}{\|x\|_X}$$

Definition 4 (Ball of radius δ)
Let V be a normed space and $u \in V$. Then the open ball of radius $\delta > 0$ centered at a point $u \in V$ is defined by

$$\mathcal{B}(u, \delta) := \{v \in V : \|u - v\|_V \leq \delta\}$$

The main result about the convergence of Newton's method is as follows [17].

Theorem 1 (Local convergence)
Let V be a Banach space and $U \in V$ be a solution of problem (3.22). Assume that F is Lipschitz continuous in the ball $\mathcal{B}(U, \delta)$, i.e. that there exists $K > 0$ such that

$$\left\|\boldsymbol{F}'(\boldsymbol{v}) - \boldsymbol{F}'(\boldsymbol{z})\right\|_{L(V,V)} \leq K \|\boldsymbol{v} - \boldsymbol{z}\|_V \qquad \forall \boldsymbol{v}, \boldsymbol{z} \in \mathcal{B}(\boldsymbol{U}, \delta), \boldsymbol{v} \neq \boldsymbol{z}$$

Then there exists in correspondence $\delta' > 0$, with $\delta' \leq \delta$, such that for all $\boldsymbol{U}^0 \in \mathcal{B}(\boldsymbol{U}, \delta')$ the sequence $\{\boldsymbol{U}^k\}$ generated by (3.17) converges quadratically to $\boldsymbol{U}$, i.e. there exists $C > 0$ such that, for a suitable $k_0 \geq 0$, we have

$$\left\|\boldsymbol{U} - \boldsymbol{U}^{k+1}\right\|_V \leq C \left\|\boldsymbol{U} - \boldsymbol{U}^k\right\|_V^2 \qquad \forall k \geq k_0$$

As previously mentioned, the use of Newton's method on the whole system (3.13) has numerous disadvantages, however it can be conveniently applied to the solution of the Poisson equation (3.9).
As proposed by Gummel in [5], setting the reference number density n_{ref}, we define the *electrochemical potential* φ_i^{ec} as

$$\varphi_i^{ec} = \varphi + \frac{V_{th}}{z_i} \ln\left(\frac{n_i}{n_{ref}}\right) \tag{3.19}$$

Then, inverting the equation for n_i, we obtain

$$n_i = n_{ref} e^{z_i\left(\varphi_i^{ec} - \varphi\right)/V_{th}} \tag{3.20}$$

and replacing (3.20) in (3.9) we obtain

$$-\nabla \cdot (\varepsilon \nabla \varphi) = q\left(\sum_{i=1}^{n} z_i n_{ref}\ e^{z_i\left(\varphi_i^{ec} - \varphi\right)/V_{th}} + \mathcal{P}\right) \tag{3.21}$$

which explicitely reveals the nonlinearity of the Poisson equation with respect to φ.

Equation (3.21) equipped by suitable boundary conditions can be represented in abstract as form

$$N(\varphi) = 0 \tag{3.22}$$

$N(\cdot)$ being a second-order semi linear differential operator. Given a tolerance $toll_{NLP} > 0$ the steps to solve the nonlinear Poisson equation (3.21) with the Newton method are shown in Figure 3.3(which corresponds to the "Poisson" boxe in Figure 3.1 and 3.2).

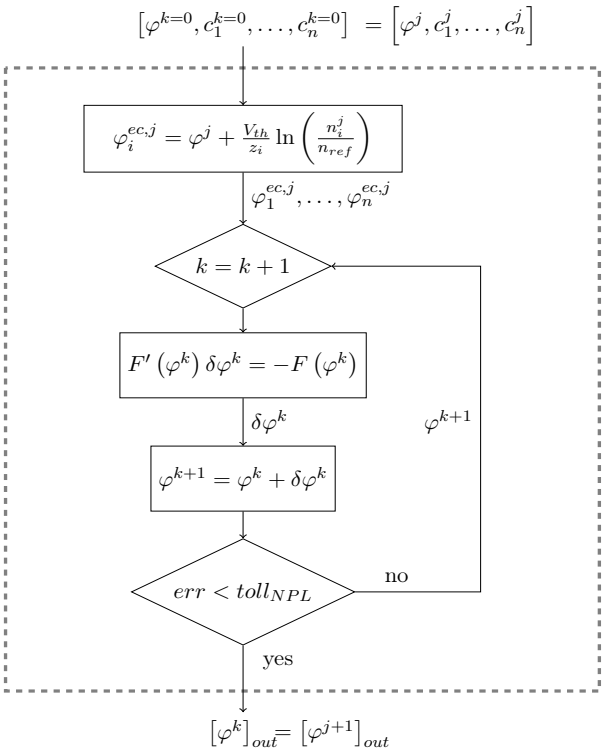

Figure 3.3: Newton scheme to solve the nonlinear Poisson equation

Some other different methods can be adopted for the solution of the Poisson equation (3.9), the easiest and most immediate is the direct linearization of the equation which allows the calculation of the electric potential φ at the

Gummel step $j+1$ using the number density $n_1, \ldots, n_n$ at the step j.

$$-\nabla \cdot \left(\varepsilon \nabla \varphi^{j+1}\right) = q\left(\sum_{i=1}^{n} z_i n_i^j + P\right) \tag{3.23}$$

This method, despite being the simplest and computationally cheapest, completely fails at incorporating the nonlinear characteristics of the Poisson equation and does not provide an effective and convergent algorithm (see [14]).

Chapter 4

Weak formulation

This chapter deals with the weak formulation of the equations of the Poisso-Maxwell-Stefan model (3.13) and their well-posedness analysis. Theorems regarding the existence and uniqueness of strong and weak solutions are proposed for the Maxwell-Stefan relations. We refer to [19] for all the definitions of functional spaces used in this chapter and their theoretical properties.

4.1 Nonlinear Poisson Equation

The application of the Newton method (3.17)-(3.18) to the nonlinear Poisson equation (3.21) leads to solving the following linearized boundary-value problem.

$$\begin{cases} \nabla \cdot \left(-\varepsilon \nabla \delta\varphi^k\right) + q\ n_{ref} \displaystyle\sum_{i=1}^{n} \frac{z_i^2}{V_{Th}}\ e^{z_i\left(\varphi_i^{ec}-\varphi^k\right)/V_{Th}} \delta\varphi^k \\ \qquad\qquad = q\ n_{ref} \displaystyle\sum_{i=1}^{n} z_i\ e^{z_i\left(\varphi_i^{ec}-\varphi^k\right)/V_{Th}} \\ \qquad\qquad\qquad + \nabla \cdot \left(-\varepsilon \nabla \varphi^k\right) + qP \qquad \text{in } \Omega \qquad (4.1a) \\ \delta\varphi^k = 0 \qquad \text{on } \partial\Omega \qquad (4.1b) \\ \varphi^{k+1} = \varphi^k + \delta\varphi^k \qquad (4.1c) \end{cases}$$

System (4.1) is a diffusion-reaction problem, with respect to the variable $\delta\varphi^k$, in Ω. Multiplying (4.1a) by a test function $\psi \in H_0^1(\Omega)$ and integrating over the domain Ω, we can state the weak formulation for the system (4.1).

To simplify the notation, we set:

$$b^k = +q\ n_{ref} \sum_{i=1}^{n} \frac{z_i^2}{V_{Th}} e^{z_i\left(\varphi_i^{ec}-\varphi^k\right)/V_{Th}}$$

and

$$f^k = \nabla \cdot \left(-\varepsilon \nabla \varphi^k\right) + q n_{ref} \sum_{i=1}^{n} z_i \exp^{z_i\left(\varphi_i^{ec}-\varphi^k\right)/V_{Th}} + qP$$

Weak formulation 1 (Nonlinear Poisson equation)
Find $\delta\varphi^k \in H_0^1(\Omega)$ *such that*

$$\int_\Omega \varepsilon\ \nabla\delta\varphi^k\ \nabla\psi\ d\Omega + \int_\Omega b^k \delta\varphi^k \psi\ d\Omega = \int_\Omega f^k \psi\ d\Omega \qquad \forall\psi \in H_0^1(\Omega) \quad (4.2)$$

In order to prove the existence and uniqueness of the solution of (4.2), we resort to the *Lax-Milgram theorem* [19].

We define the bilinear form:

$$a : H_0^1(\Omega) \times H_0^1(\Omega) \to \mathbb{R}, \qquad a(\varphi,\psi) = \int_\Omega \varepsilon \nabla\varphi\nabla\psi\ d\Omega + \int_\Omega b^k\varphi\psi\ d\Omega \quad (4.3)$$

and the linear functional

$$F : H_0^1(\Omega) \to \mathbb{R}, \qquad F(\psi) = \int_\Omega f^k \psi\ d\Omega \quad (4.4)$$

We set:

$$\varepsilon_M = \max_\Omega(\varepsilon) \qquad b_M^k = \max_\Omega\left(b^k\right)$$
$$\varepsilon_m = \min_\Omega(\varepsilon) \qquad b_m^k = \min_\Omega\left(b^k\right)$$

and we have:

- **Continuity of the bilinear form** $a(\cdot,\cdot)$

$$\begin{aligned}\int_\Omega \varepsilon\nabla\phi\ \nabla\psi\ d\Omega + \int_\Omega b^k\varphi\psi\ d\Omega &\le \varepsilon_M \|\nabla\varphi\|_{L^2} \|\nabla\psi\|_{L^2} + b_M^k \|\varphi\|_{L^2} \|\psi\|_{L^2} \\ &\le \max\left(\varepsilon_M, b_M^k\right) \|\varphi\|_{H_0^1} \|\psi\|_{H_0^1} \\ &\le C \|\varphi\|_{H_0^1} \|\psi\|_{H_0^1} \qquad \forall\varphi,\psi\ \in H_0^1(\Omega)\end{aligned}$$

- **Coercivity of the bilinear form** $a(\cdot,\cdot)$

$$\begin{aligned}\int_\Omega \varepsilon\ (\nabla\varphi)^2\ d\Omega + \int_\Omega b^k\varphi^2\ d\Omega &\geq \varepsilon_m \|\nabla\varphi\|_{L^2}^2 + b_m^k \|\varphi\|_{L^2}^2 \\ &\geq \varepsilon_m \|\nabla\varphi\|_{L^2}^2 \\ &= \varepsilon_m \|\varphi\|_{H_0^1}^2 \qquad\qquad \forall\varphi \in H_0^1(\Omega)\end{aligned}$$

- **Continuity of the linear functional** $F(\cdot)$

$$\begin{aligned}\int_\Omega f^k\psi\ d\Omega &\leq \left\|f^k\right\|_{L^2} \|\psi\|_{L^2} \\ &\leq \left\|f^k\right\|_{L^2} \|\psi\|_{H_0^1} \qquad \forall\psi \in H_0^1(\Omega)\end{aligned}$$

Thus $\forall k \geq 0$ there exists a unique weak solution of the linearized boundary value problem (4.1).

4.2 Continuity equations and Maxwell-Stefan relations

As anticipated in chapter 3, the analysis and solution of the equation systems (3.13a) and (3.13b) is not an easy task. However, some important results exist in literature[1][10]; some of them are shown below to provide a complete picture of the topic.

Theorem 2 (Existence and uniqueness, locally in time, of a strong solution) *Let $\Omega \in \mathbb{R}^N$, with $N \geq 1$, be open bounded with smooth $\partial\Omega$. Let $p \geq \frac{N+2}{2}$ and $u_0 \in W_p^{2-2/p}(\Omega; E)$ such that $c_i^0 \geq 0$ in $\bar{\Omega}$ and c_t^0 is constant in Ω. Let the diffusion matrix $\boldsymbol{D}(u)$ given by*

$$\boldsymbol{D}(u) = X^{\frac{1}{2}} \left(A_{S|\hat{E}}\right)^{-1} X^{\frac{1}{2}} G''(\boldsymbol{x}) \ \text{ with } c_t x_i = u_i + c_t^0/n$$

where $G : (0,+\infty)^n \to \mathbb{R}$ is smooth and strongly convex. Then there exists - locally in time - a unique strong solution (in the L^p sense) of

$$\begin{aligned}&\partial_t u + \nabla\cdot(-\boldsymbol{D}(u)\nabla u) = 0 \\ &\partial_\nu u\,|_{\partial\Omega} = 0 \\ &u\,|_{t=0} = u_0\end{aligned}$$

This solution is in fact classical.

Theorem 3 (Existence of a weak solution)
Let:

- $\Omega \subset \mathbb{R}^d$, $d \leq 3$, *be a bounded domain with* $\partial\Omega \in C^{1,1}$;
- $c_1^0, \ldots, c_{n-1}$ $(n \geq 3)$ *be nonnegative functions such that*

$$c_n^0 = 1 - \sum_{i=1}^{n-1} c_i^0 \qquad \text{and} \qquad \sum_{i=1}^{n-1} c_i^0 \leq 1$$

- $\mathrm{Đ} \in \mathbb{R}^{n\times n}$ *a symmetric matrix with elements* $\mathrm{Đ}_{ij} > 0$ *for* $i \neq j$;
- $r_i \in C^0\left([0,1]^n; \mathbb{R}\right)$, *for* $i = 1, \ldots, n$ *satisfying*

$$\sum_{i=1}^{n} r_i(\boldsymbol{c}) \qquad \sum_{i=1}^{n} r_i(\boldsymbol{c}) \log c_i \leq 0 \qquad \forall 0 < c_1, \ldots, c_n <\leq 1$$

Then there exists a weak solution $(c_1, \ldots, c_n)$ *to*

$$\begin{cases} \partial_t c_i + \nabla \cdot N_i = r_i(\boldsymbol{c}) & & \text{(4.5a)} \\ \nabla x_i = -\displaystyle\sum_{\substack{j=1 \\ j\neq i}}^{n} \frac{x_j \boldsymbol{N}_i - x_i \boldsymbol{N}_j}{c_t\ \mathrm{Đ}_{ij}} & & \text{(4.5b)} \\ \nabla c_i \cdot \nu = 0 & \text{on } \partial\Omega & \text{(4.5c)} \\ c_i(\cdot, 0) = c_i^0 & \text{in } \Omega & \text{(4.5d)} \end{cases}$$

such that $c_i \in L^2_{loc}\left(0, \infty; H^1(\Omega)\right)$ *and* $\partial_t c_i \in L^2_{loc}\left(0, \infty; \mathcal{V}'(\Omega)\right)$ *satisfying*

$$0 \leq c_i \leq 1 \quad i = 1, \ldots, n-1 \qquad c_n = 1 - \sum_{i=1}^{n-1} c_i \geq 0 \quad \text{in } \Omega, t > 0$$

where $\mathcal{V}'$ *is the dual space of* $\mathcal{V} = \left\{u \in H^2(\Omega) : \nabla u \cdot \nu = 0 \text{ on } \partial\Omega\right\}$.

For system (4.5) with $r = (r_1, \ldots, r_n)^T = 0$, the following result holds:

Theorem 4 (Exponential decay)
Let the assumptions of Theorem 3 hold. We suppose $r = 0$ *and* $\min_{i=1,\ldots,n} \left\|c_i^0\right\|_{L^1(\Omega)} > 0$. *Let* $(c_1, \ldots, c_n)$ *be the weak solution constructed in Theorem 3 and define*

$c^0 = \left(c_1^0, \ldots, c_n^0\right)^T$. *Then there exist two constants* $C > 0$, *depending only on* Ω, *and* $\lambda > 0$, *depending only on* Ω *and* Đ, *such that*

$$\left\|c_i\left(\cdot, t\right) - \bar{c}_i^0\right\|_{L^1(\Omega)} \leq Ce^{-\lambda t}\sqrt{\mathcal{H}\left(c^0\right)} \qquad i = 1, \ldots, n$$

where

$$\mathcal{H}\left(c\right) = \sum_{i=1}^{n} \int_\Omega c_i \log \frac{c_i}{\bar{c}_i^0}\, d\Omega$$

and

$$\bar{c}_i^0 = |\Omega|^{-1} \int_\Omega c_i^0\, d\Omega$$

Furthermore $\left(\bar{c}_1^0, \ldots, \bar{c}_n^0\right)^T$ *is a homogeneous steady state of* (4.5).

For further results, see also [2],[4] and [7].

In order to solve equations (3.13a) and (3.13b) using the Gummel Map as in the scheme of Figure 3.2, we proceed with their linearization. Let x_i^j and $\boldsymbol{N}_i^j$ be the molar fractions and the molar fluxes computed at the $j-th$ step of the Gummel Map, then x_i^{j+1} and $\boldsymbol{N}_i^{j+1}$ are obtained by solving:

$$\begin{cases} c_t \dfrac{\partial x_i^{j+1}}{\partial t} + \nabla \cdot \boldsymbol{N}_i^{j+1} = 0 & \text{in } Q_T \quad (4.6a) \\ \displaystyle\sum_{\substack{k=1 \\ j \neq i}}^{n} \frac{x_k^j \boldsymbol{N}_i^j - x_i^{j+1} \boldsymbol{N}_k^j}{c_t \text{Đ}_{i,k}} + \sum_{\substack{k=1 \\ k \neq i}}^{n} \frac{x_i^{j+1} x_k^j \left(\alpha_i - \alpha_k\right)}{\text{Đ}_{i,k}} \frac{\nabla T}{T} & \\ \qquad = -\nabla x_i^{j+1} - \dfrac{z_{i,eff}^j \mathcal{F}}{RT} x_i^{j+1} \nabla \varphi^{j+1} & \text{in } Q_T \quad (4.6b) \\ x_i^0(\cdot, 0) = \bar{x}_i(\cdot) & \text{in } \Omega \quad (4.6c) \\ \boldsymbol{N}_i^{j+1} \cdot \nu = 0 & \text{on } S_T \quad (4.6d) \end{cases}$$

Let us introduce μ_i^j and a_i^j (see Section 5.3.3) such that

$$\boldsymbol{N}_i^{j+1} = -\mu_i^j \nabla x_i^{j+1} + a_i^j x_i^{j+1} \tag{4.7}$$

where $\mu_i^j = \mu_i^j\left(x_i^j\right)$ and $a_i^j = a_i^j\left(x_i^j, \boldsymbol{N}_i^j, \varphi^j\right)$.

System (4.6) is a set of $n-1$ advection-diffusion equations, with respect to the variables x_i for $i = 1, \dots, n-1$, in Q_T. Including (4.7) in (4.6a) and multiplying it by a test function $\psi \in H^1(\Omega)$ and integrating over all the domain Ω, we can state the weak formulation for system (4.6).

Weak formulation 2 (Continuity and Maxwell-Stefan equations)
Find $x_i^{j+1} \in L^2\left(0,T;H^1\right)$ *such that* $\dot{x}_i^{j+1} \in L^2\left(0,T;\left(H^1\right)^*\right)$ *and*

1. $\forall \psi \in H^1(\Omega)$, *a.e. in* $t \in [0,T]$

$$\int_\Omega c_t \frac{\partial x_i^{j+1}}{\partial t} \psi \, d\Omega + \int_\Omega \mu_i^j \nabla x_i^{j+1} \nabla \psi \, d\Omega - \int_\Omega a_i^j x_i^{j+1} \nabla \psi \, d\Omega = 0 \quad (4.8)$$

2.
$$c_i^0(\cdot, 0) = \bar{c}_i(\cdot) \qquad \text{in } \Omega$$

where $\left(H^1\right)^*$ *is the dual space of* H^1.

We define the bilinear form:

$$a : H^1(\Omega) \times H^1(\Omega) \to \mathbb{R}, \; a(\varphi, \psi) = \int_\Omega \mu \nabla \varphi \nabla \psi \, d\Omega - \int_\Omega a \varphi \nabla \psi \, d\Omega \quad (4.9)$$

Since $Đ_{ij} > 0$ for an ideal mixture, given $\bar{c}_{1,\dots,n} \in L^\infty(\Omega)$, it is possible to prove (see Section 5.3.3) that $\mu_i^j > 0$ and $\mu_i^j \in L^\infty(\Omega)$ for all i and j. Moreover we assume that also $a_i^j \in L^\infty(\Omega)$ for all i and j. In order to prove the existence and uniqueness of the solution of (4.8), we resort to the analogous of the *Lax-Milgram theorem* for parabolic equations [19].

We set:

$$\mu_M = \max_\Omega(\mu) \qquad a_M = \max_\Omega(|a|)$$
$$\mu_m = \min_\Omega(\mu) \qquad a_m = \min_\Omega(|a|)$$

The existence and uniqueness of the weak solution is guaranteed by the following steps:

- **Continuity of the bilinear form** $a(\cdot,\cdot)$

$$\begin{aligned} \int_\Omega \mu \nabla \phi \, \nabla \psi \, d\Omega - \int_\Omega a \, \varphi \nabla \psi \, d\Omega \quad &\leq \mu_M \|\nabla \varphi\|_{L^2} \|\nabla \psi\|_{L^2} + a_M \|\varphi\|_{L^2} \|\nabla \psi\|_{L^2} \\ &\leq \max(\mu_M, a_M) \|\varphi\|_{H^1} \|\nabla \psi\|_{L^2} \\ &\leq C \|\varphi\|_{H^1} \|\psi\|_{H^1} \qquad \forall \varphi, \psi \in H^1(\Omega) \end{aligned}$$

- **Weak-coercivity of the bilinear form** $a(\cdot,\cdot)$
  Let us consider separately the two integrals in the bilinear form $a(\cdot,\cdot)$.

$$\int_\Omega \mu \ (\nabla\varphi)^2 \ d\Omega \geq \mu_m \|\nabla\varphi\|_{L^2}^2 \tag{4.10}$$

$$\int_\Omega a \ \varphi \ \nabla\varphi \ d\Omega \leq \ a_M \|\nabla\varphi\|_{L^2} \|\varphi\|_{L^2} \tag{4.11}$$

  Then, using the well-known inequality

$$2ab \leq \varepsilon \ a^2 + \frac{1}{\varepsilon} \ b^2 \qquad \forall \ a, b, \in \mathbb{R}, \ \varepsilon > 0$$

  and choosing $\varepsilon = \frac{\mu_m}{a_M}$, inequality (4.11) becomes

$$\begin{aligned} -\int_\Omega a \ \varphi \ \nabla\varphi \ d\Omega &\geq - \ a_M \|\nabla\varphi\|_{L^2} \|\varphi\|_{L^2} \\ &\geq -\frac{a_M}{2} \left(\frac{\mu_m}{a_M} \|\nabla\varphi\|_{L^2}^2 + \frac{a_M}{\mu_m} \|\varphi\|_{L^2}^2 \right) \end{aligned} \tag{4.12}$$

  Combining the results in (4.10) and (4.12) we obtain

$$a(\varphi,\varphi) + \lambda \|\varphi\|_{L^2}^2 \geq \frac{\mu_m}{2} \|\nabla\varphi\|_{L^2}^2 - \frac{a_M^2}{2\mu_m} \|\varphi\|_{L^2}^2 + \lambda \|\varphi\|_{L^2}^2 \qquad \forall \ \lambda > 0$$

  Then, choosing $\lambda = \frac{a_M^2}{\mu_m}$, we get the weak coercivity of the bilinear form $a(\cdot,\cdot)$

$$a(\varphi,\varphi) + \lambda \|\varphi\|_{L^2}^2 \geq \min\left(\frac{\mu_m}{2}, \frac{\lambda}{2} \right) \|\varphi\|_{H^1}^2 \qquad \forall \varphi \in H^1$$

Chapter 5

Galerkin Finite Element Approximation

In this chapter we discuss the numerical approximation of equations (4.2) and (4.8) according to the *Galerkin method*, and then we proceed with the discretization of the resulting problem through the *Finite Element Method* (FEM).

5.1 Galerkin method

The weak formulation of the Poisson equation (4.2) can be represented in compact form as:

Find $u \in V$ *such that*

$$a(u, v) = F(v) \qquad \forall v \in V \tag{5.1}$$

In Section 4.1, we considered $V = H^1(\Omega)$.
Let V_h be a finite-dimentional subspace of V, depending on $h > 0$, such that

$$dim(V_h) < \infty \text{ and } V_h \subset V \qquad \forall h > 0$$

The Galerkin formulation of (5.1) reads:

Find $u_h \in V_h$ *such that*

$$a(u_h, v_h) = F(v_h) \qquad \forall v_h \in V_h \tag{5.2}$$

The well-posedness of problem (5.2) is a direct consequence of the analysis carried out in Section 4.1.

Defining the *Hilbert triplet* (V, H, V^*), the weak formulation of (4.8) can be represented in compact form as:

Given $g \in H$, *find* $u \in L^2(0,T;V)$ *such that* $\dot{u} \in L^2(0,T;V^*)$ *and that*:

$$\begin{aligned} (\dot{u}(t), v)_V + a(u(t), v; t) &= 0 \qquad \forall v \in V \\ u(0) &= g \end{aligned} \tag{5.3}$$

In Section 4.2, we consider $V = H^1(\Omega)$, $H = L^2(\Omega)$ and $V^* = \left(H^1\right)^*(\Omega)$. Let V_h,H_h,V_h^*, depending on $h > 0$, be a triplet of finite-dimentional subspaces of V,H,V^* such that:

$$\begin{aligned} &dim(V_h) < \infty \quad \text{and} \quad V_h \subset V \quad \forall h > 0 \\ &dim(H_h) < \infty \quad \text{and} \quad H_h \subset H \quad \forall h > 0 \\ &dim(V_h^*) < \infty \quad \text{and} \quad V_h^* \subset V^* \quad \forall h > 0 \end{aligned}$$

The Galerkin formulation of (5.3) reads:

Given $g_h \in H_h$, *find* $u_h \in L^2(0,T;V_h)$ *such that* $\dot{u_h} \in L^2(0,T;V_h^*)$ *and that*:

$$\begin{aligned} (\dot{u}_h(t), v_h)_{V_h} + a(u_h(t), v_h; t) &= 0 \qquad \forall v_h \in V_h \\ u_h(0) &= g_h \end{aligned} \tag{5.4}$$

The well-posedness of problem (5.4) is a direct consequence of the analysis carried out in Section 4.2.

5.2 The Finite Element Method

In this section we introduce the Finite Element Method (FEM) for its application to formulations (5.2) and (5.4).
Let $\mathcal{T}_h$ be a partition of Ω and K an element of $\mathcal{T}_h$ such that $\mathcal{T}_h = \cup K$. Let $r \geq 1$ a given integer and $V_h = X_h^r$ be the finite element space of the elementwise polynomial functions, defined as:

$$X_h^r(\Omega) := \left\{ v_h \in C^0\left(\bar{\Omega}\right) : v_h|_K \in \mathbb{P}_r(K), \forall K \in \mathcal{T}_h \right\} \tag{5.5}$$

We denote by $\{\psi_j\}_{j=1}^{N_h}$ a *Lagrangian basis* of the space X_h^r so that every function $u_h \in V_h$ can be espressed as a linear combination of $\psi_{j=1,\dots,N_h}$:

$$u_h(\boldsymbol{x}) = \sum_{j=1}^{N_h} u_j \psi_j(\boldsymbol{x}) \tag{5.6}$$

Therefore the discrete version of problem of (5.2) becomes:
Find $[u_1, \dots, u_{N_h}]^T \in \mathbb{R}^{N_h}$ *such that*

$$\sum_{j=1}^{N_h} u_j \; a(\psi_j, \psi_i) = F(\psi_i) \qquad \forall i = 1, \dots, N_h \tag{5.7}$$

Defining the matrix $\boldsymbol{A}$,

$$\boldsymbol{A} \in \mathbb{R}^{\mathcal{N}_h \times \mathcal{N}_h}, \qquad A_{ij} = a(\psi_j, \psi_i)$$

the vector $\boldsymbol{b}$

$$\boldsymbol{b} \in \mathbb{R}^{\mathcal{N}_h}, \qquad b_i = F(\psi_i)$$

and the vector $\boldsymbol{u}$

$$\boldsymbol{u} = [u_1, \dots, u_{N_h}]^T$$

system (5.7) can be written in matrix form as:

$$\boldsymbol{A}\boldsymbol{u} = \boldsymbol{b} \tag{5.8}$$

With a similar procedure, we obtain that every function $u_h \in V_h$ is a linear combination of the Lagrangian basis $\psi_{j=1,\dots,N_h}$

$$u_h(\boldsymbol{x}, t) = \sum_{j=1}^{N_h} u_j(t) \psi_j(\boldsymbol{x}) \tag{5.9}$$

and the coefficients $u_{j=1,\dots,N_h}$ are time dependent functions.

The semi-discrete formulation of (5.4) reads:

Find $[u_1(t), \dots, u_{N_h}(t)]^T \in \mathbb{R}^{N_h}$ *such that*

$$\sum_{j=1}^{N_h} \dot{u}_j(t) \int_\Omega \psi_j \psi_i \, d\Omega + \sum_{j=1}^{N_h} u_j(t) \; a(\psi_j, \psi_i) = 0 \qquad \forall i = 1, \dots, N_h \tag{5.10}$$

Defining the matrix $\boldsymbol{A}$,

$$\boldsymbol{A} \in \mathbb{R}^{\mathcal{N}_h \times \mathcal{N}_h}, \qquad A_{ij} = a(\psi_j, \psi_i)$$

the matrix $\boldsymbol{M}$

$$\boldsymbol{M} \in \mathbb{R}^{\mathcal{N}_h \times \mathcal{N}_h}, \qquad M_{ij} = \int_\Omega \psi_j \psi_i \, d\Omega$$

and the vector $\boldsymbol{u}$

$$\boldsymbol{u} = [u_1(t), \dots, u_{N_h}(t)]^T$$

system (5.10) can be written in matrix form as:

$$\boldsymbol{M}\dot{\boldsymbol{u}}(t) + \boldsymbol{A}\boldsymbol{u}(t) = 0 \tag{5.11}$$

The time discretization of (5.11) can be performed using the *ϑ-method*.

$$\boldsymbol{M}\frac{\boldsymbol{u}^{k+1} - \boldsymbol{u}^k}{\Delta t} + \boldsymbol{A}\left[\theta \boldsymbol{u}^{k+1} + (1-\theta)\boldsymbol{u}^k\right] = 0 \tag{5.12}$$

where $\vartheta \in [0, 1]$ is a parameter.
The most relevant cases are:

- $\theta = 0$ yielding the *forward Euler method*

$$\boldsymbol{M}\frac{\boldsymbol{u}^{k+1} - \boldsymbol{u}^k}{\Delta t} + \boldsymbol{A}\boldsymbol{u}^k = 0 \tag{5.13}$$

  that is a first-order accurate method with respect to Δt;

- $\theta = 1$ yielding the *backward Euler method*

$$\boldsymbol{M}\frac{\boldsymbol{u}^{k+1} - \boldsymbol{u}^k}{\Delta t} + \boldsymbol{A}\boldsymbol{u}^{k+1} = 0 \tag{5.14}$$

  that is a first-order accurate method;

- $\theta = \frac{1}{2}$ yielding the *Crank-Nicolson method*

$$\boldsymbol{M}\frac{\boldsymbol{u}^{k+1} - \boldsymbol{u}^k}{\Delta t} + \frac{1}{2}\boldsymbol{A}\left(\boldsymbol{u}^{k+1} + \boldsymbol{u}^k\right) = 0 \tag{5.15}$$

  that is a second-order accurate method;

5.3 Implementation

This section discusses the solution of problems (5.2) and (5.4), set in a one-dimensional domain, using the finite element method. Let $\Omega = (a, b) \subset \mathbb{R}$ be a one-dimentional domain and $\mathcal{T}_h$ a partition of Ω composed of N_ξ intervals of size $\Delta\xi_i$

$$\Delta\xi_i = \xi_i - \xi_{i-1} \qquad \forall i = 1, \dots, N_\xi$$

If the grid intervals are uniform, i.e. $\Delta\xi_i = \Delta\xi_j \ \forall i, j = 1, \dots, N_\xi$, they are indicated with $\Delta\xi$. Moreover, let us choose $V_h = X_h^1(\Omega)$ and its *Lagrangian basis* $\{\psi_k\}_{k=1}^{N_\xi}$.

$$\psi_k = \begin{cases} \dfrac{x - x_{i-1}}{x_i - x_{i-1}} & \text{for} \quad x_{i-1} \le x \le x_i \\ \dfrac{x_{i+1} - x}{x_{i+1} - x_i} & \text{for} \quad x_i \le x \le x_{i+1} \\ 0 & \text{otherwise} \end{cases} \tag{5.16}$$

$$\psi_k(x_j) = \delta_{k,j} \qquad k, j = 0, \dots, N_\xi$$

Following the theory of Section 5.2, the discretization of the initial data $c_i(\xi, 0)$ in (3.13g) on the X_h^1 space reads

$$c_{h,i}(\xi, 0) = \sum_{j=1}^{N_\xi} c_i(\xi_j, 0)\psi_j(\xi)$$

where $c_i(\xi_j, 0)$ are the evaluations of the functions c_i at time $t = 0$ at the temporal grid nodes ξ_j. By (2.1a) and the equimolar constraint it follows that

$$c_{h,t}(\xi) = \sum_{j=1}^{N_\xi} c_t(\xi_j)\psi_j(\xi) = \sum_{j=1}^{N_\xi} \sum_{i=1}^{n} c_i(\xi_j, 0)\psi_j(\xi)$$

where $c_t(\xi_j, 0)$ are the evaluations of the function c_t at the temporal grid nodes ξ_j.
The discretization of the molar fraction x_i reads

$$x_i(\xi) = \sum_{j=1}^{N_\xi} x_i(\xi_j)\psi_j(\xi) = \sum_{j=1}^{N_\xi} \frac{c_i(\xi_j, 0)}{c_t(\xi_j)}\psi_j(\xi)$$

5.3.1 Linearzation of the NLP equation

Following the solution scheme described in Figure 3.1, the electric potential is evaluated by applying the Newton method applied to the to the Nonlinear Poisson equation (for details see Section 3.4.2 and Figure 3.3). Let us focus on some interesting aspects of the linearization procedure.

The bilinear form (4.3)

$$a\left(\psi_j, \psi_i\right) = \int_\Omega \varepsilon \ \nabla\psi_j \ \nabla\psi_i \ d\Omega + \int_\Omega b^k \psi_j \psi_i \ d\Omega$$

is composed of two integrals. The first one refers to the diffusive contribution and generates the so-called *stiffness matrix*, while the second is concerned to the reaction term and generates the *mass matrix*.

The permittivity ε is a characteristic medium quantity; since the mixture changes its composition locally according to the $n-1$ continuity-Maxwell-Stefan equations it is reasonable to suppose that ε is a function of the molar fractions x_i. However, for simplicity, we consider ε as a piecewise constant function on $\mathcal{T}_h$, thus the computation of the first integral in (4.3) is extremely simple.

On the other side the function b^k can not be considered piecewise constant, so it is necessary to resort to numerical integration techniques. The choice of the discrete space X_h^1 imposes a first order convergence rate in $\|\cdot\|_1$ with respect to h. This implies that the trapezoidal rule is enough accurate and higher order quadrature rule than the first order is not needed. Using trapeziodal quadrature rule the mass-matrix becomes diagonal. This technique is known as *lumping procedure*.

The algebraic formulation of the Linearized Nonlinear Poisson equation (4.2) at each Newton iteration reads:

$$\begin{cases} \boldsymbol{A}^k \delta\varphi^k = \boldsymbol{b}^k \\ \varphi^{k+1} = \varphi^k + \delta\varphi^k \end{cases} \tag{5.17}$$

5.3.2 Fluxes

The next step in the solution scheme described in Figure 3.1 is the computation of fluxes. Assuming the electric potential φ to be a known function,

the molar fractions x_i and the $n-1$ fluxes $\boldsymbol{N}_i$ can be obtained from the Maxwell-Stefan equations as follows. Let us consider the $n-1$ equations (3.13b). Imposing constraints (3.13d) and (3.13e) we obtain

$$\begin{aligned}
-\nabla x_i \quad &= \left(\sum_{\substack{j=1 \\ j\neq i}}^{n-1} \frac{1}{c_t \text{Đ}_{ij}} x_j + \left(1 - \sum_{\substack{j=1 \\ j\neq i}}^{n-1} x_j \right) \right) \boldsymbol{N}_i + \sum_{\substack{j=1 \\ j\neq i}}^{n-1} \left(\frac{1}{c_t \text{Đ}_{in}} - \frac{1}{c_t \text{Đ}_{ij}} \right) x_i \boldsymbol{N}_j \\
&+ \sum_{\substack{j=1 \\ j\neq i}}^{n-1} \frac{1}{\text{Đ}_{ij}} x_i x_j \left(\alpha_i - \alpha_j \right) \frac{\nabla T}{T} + \frac{1}{\text{Đ}_{in}} x_i \left(1 - \sum_{j=1}^{n-1} x_j \right) \left(\alpha_i - \alpha_n \right) \frac{\nabla T}{T} \\
&+ \frac{z_{i,eff} \mathcal{F}}{R\, T} x_i \nabla \varphi
\end{aligned}$$

that after some algebra can be rewritten as

$$\begin{aligned}
\sum_{\substack{j=1 \\ j\neq i}}^{n-1} \left(\frac{1}{\text{Đ}_{in}} - \frac{1}{\text{Đ}_{ij}} \right) x_i \boldsymbol{N}_j + \left(\frac{1}{\text{Đ}_{in}} + \sum_{\substack{j=1 \\ j\neq i}}^{n-1} \left(\frac{1}{\text{Đ}_{ij}} - \frac{1}{\text{Đ}_{in}} \right) x_j \right) \boldsymbol{N}_i & \\
= c_t \left(- \sum_{\substack{j=1 \\ j\neq i}}^{n-1} \frac{x_i x_j}{\text{Đ}_{ij}} \left(\alpha_i - \alpha_j \right) \frac{\nabla T}{T} \right. & \\
- \frac{x_i}{\text{Đ}_{in}} \left(1 - \sum_{j=1}^{n-1} x_j \right) \left(\alpha_i - \alpha_n \right) \frac{\nabla T}{T} & \\
\left. - \frac{z_{i,eff} \mathcal{F}}{R\, T} x_i \nabla \varphi - \nabla x_i \right) &
\end{aligned} \tag{5.18}$$

or, alternatively, introducing the matrix $\boldsymbol{A}(x)$, the vector of the unknowns $\boldsymbol{n}$ and the vector of the known terms $\boldsymbol{b}(x, \varphi)$, can be formulated as

$$\boldsymbol{A}(x)\, \boldsymbol{n} = \boldsymbol{b}(x, \varphi) \tag{5.19}$$

where

$$\boldsymbol{A}_{i,j}(x) = \frac{1}{Đ_{in}} + \sum_{\substack{j=1 \\ j\neq i}}^{n-1} \left(\frac{1}{Đ_{ij}} - \frac{1}{Đ_{in}}\right) x_j \qquad i = j$$

$$\boldsymbol{A}_{i,j}(x) = \left(\frac{1}{Đ_{in}} - \frac{1}{Đ_{ij}}\right) x_i \qquad \text{otherwise}$$

and $\boldsymbol{n} = [\boldsymbol{N}_1, \ldots, \boldsymbol{N}_{n-1}]^T$ and $b_i(x, \varphi)$ is the right hand side of (5.18) for every i. Since Ω is a 1D domain, the $\boldsymbol{N}_i$ fluxes are reduced to the scalar functions N_i. Let us define every discrete flux function $N_{h,i}(\xi, 0)$ as a linear combination of the basis functions (5.16)

$$N_{h,i}(\xi, 0) = \sum_{j=1}^{N_\xi} N_i(\xi_j, 0)\psi_j(\xi)$$

Then, the $N_i(\xi_j, 0)$ coefficients are obtained by solving system (5.19) evaluated at each mesh node and setting $x_i = x_i^0$ and $\varphi = \varphi^0$. The discrete flux function $N_{h,n}(\xi, 0)$ is computed using the equimolar constraint (3.13e).

5.3.3 Continuity Maxwell-Stefan equation

Proceeding along the solution scheme in Figure 3.1 we arrive at the time steps, and inside them, to the Gummel map in Figure 3.2. The Linearized Nonlinear Poisson equation has already been discussed in Section 5.3.1, so that we now turn to the analysis of the Maxwell-Stefan continuity equations (4.8).

In Section 4.7 we have introduced μ_i and a_i such that each flux function $\boldsymbol{N}_i$ may be written as

$$\boldsymbol{N}_i = -\mu_i \nabla x_i + a_i x_i$$

From equation (5.18), leaving only $\boldsymbol{N}_i$ to the lhs, it is easy to see that

$$\mu_i = c_t \left(\frac{1}{Đ_{in}} + \sum_{\substack{j=1 \\ j\neq i}}^{n-1} \left(\frac{1}{Đ_{ij}} - \frac{1}{Đ_{in}}\right) x_j\right)^{-1} \tag{5.20}$$

and

$$
\begin{aligned}
a_i = \Bigg(& \sum_{\substack{j=1 \\ j\neq i}}^{n-1} \left(\frac{1}{\mathfrak{D}_{ij}} - \frac{1}{\mathfrak{D}_{in}} \right) \boldsymbol{N}_j \\
& - \sum_{\substack{j=1 \\ j\neq i}}^{n-1} \frac{1}{\mathfrak{D}_{ij}} x_j \left(\alpha_i - \alpha_j \right) \frac{\nabla T}{T} \\
& - \frac{1}{\mathfrak{D}_{in}} \left(1 - \sum_{j=1}^{n-1} x_j \right) \left(\alpha_i - \alpha_n \right) \frac{\nabla T}{T} \\
& - \frac{z_{i,eff} \mathcal{F}}{R\, T} \nabla \varphi \Bigg) \left(\frac{1}{\mathfrak{D}_{in}} + \sum_{\substack{j=1 \\ j\neq i}}^{n-1} \left(\frac{1}{\mathfrak{D}_{ij}} - \frac{1}{\mathfrak{D}_{in}} \right) x_j \right)^{-1}
\end{aligned}
\tag{5.21}
$$

If the molar concentrations $c_i(\cdot, 0) \in L^\infty(\Omega)\ \ \forall i = 1, \ldots, n$, then $c_t \in L^\infty(\Omega)$ since it is a finite sum of $L^\infty(\Omega)$ functions. Furthermore, since the following inequalities hold:

$$
\frac{1}{\mathfrak{D}_{in}} + \sum_{\substack{j=1 \\ j\neq i}}^{n-1} \left(\frac{1}{\mathfrak{D}_{ij}} - \frac{1}{\mathfrak{D}_{in}} \right) x_j = \frac{(x_i + x_n)}{\mathfrak{D}_{in}} + \sum_{\substack{j=1 \\ j\neq i}}^{n-1} \frac{x_j}{\mathfrak{D}_{ij}} \leq \max_{j\neq i} \left(\frac{1}{\mathfrak{D}_{ij}} \right) \tag{5.22a}
$$

and

$$
\frac{1}{\mathfrak{D}_{in}} + \sum_{\substack{j=1 \\ j\neq i}}^{n-1} \left(\frac{1}{\mathfrak{D}_{ij}} - \frac{1}{\mathfrak{D}_{in}} \right) x_j \geq \min_{i\neq j} \left(\frac{1}{\mathfrak{D}_{ij}} \right) > 0 \tag{5.22b}
$$

we have that $\mu_i \in L^\infty(\Omega)$ for all the Gummel Map iterations and at each time level.

Let us give some details on the calculation of the $z_{i,eff}$ exploiting the defi-

nition of ω_i (2.5c)

$$\begin{aligned} z_{i,eff} &= z_i - \omega_i \sum_{j=1}^{n} \frac{z_j x_j}{x_i} = z_i - \frac{\rho_i}{\rho_t} \sum_{j=1}^{n} \frac{z_j x_j}{x_i} \\ &= z_i - \frac{c_t x_i M_i}{\sum_{j=1}^{n} c_t x_j M_j} \sum_{j=1}^{n} \frac{z_j x_j}{x_i} \\ &= z_i - \frac{M_i}{\sum_{j=1}^{n} x_j M_j} \sum_{j=1}^{n} z_j x_j \end{aligned} \tag{5.23}$$

Using the Backward Euler method (5.14) for the temporal discretization of the $n-1$ continuity Maxwell-Stefan equations, the algebraic formulation of (4.8) for each step of the Gummel Map reads

$$\frac{c_t}{\Delta t} \boldsymbol{M}\boldsymbol{u}^{j+1} + \boldsymbol{A}\boldsymbol{u}^{j+1} = \frac{c_t}{\Delta t} \boldsymbol{M}\boldsymbol{u}^{j} \tag{5.24}$$

At each iteration of the Gummel Map, μ_i and a_i are computed using the evaluation of x_i and φ at the previous Gummel iteration and of $\boldsymbol{N}_i$ at the previous time level.

Chapter 6

Simulation Tests and Comparison between Poisson-Maxwell-Stefan and Poisson-Nernst-Planck Models

The purpose of this chapter is to compare the Maxwell-Stefan model with Fick's model of diffusion (2.6) and the Poisson-Maxwell-Stefan model with the Poisson-Nernst-Planck model. Through these comparisons, we will try to identify the advantages and limitations of these models. In particular, the chapter will be divided into the following sections:

- Section 6.1: tests on the Maxwell-Stefan model with non-constant temperature and electrical potential and with several intial conditions;
- Section 6.2: comparison between the Maxwell-Stefan and Fick models;
- Section 6.3: comparison between the Poisson-Maxwell-Stefan and Poisson-Nernst-Planck models .

In this chapter all tests are performed on ternary mixtures, composed of the chemical species $S1$, $S2$ and $S3$ which have the characteristics presented in Table 6.1 (or clearly indicated in the test) and whose matrix of the diffusion coefficients of Maxwell-Stefan is Đ.

$$Đ = \begin{bmatrix} 0 & 0.033293 & 0.026117 \\ 0.033293 & 0 & 0.036936 \\ 0.026117 & 0.036936 & 0 \end{bmatrix} \tag{6.1}$$

	$S1$	$S2$	$S3$	
z_i	0.7	1	1	–
M_i	$1.2061e-25$	$2.1189e-25$	$2.019e-25$	$kg\ mol^{-1}$
D_i^T	$3.1269e-25$	$0.2783e-25$	$1.9525e-25$	$kg\ m^{-1}s^{-1}$

Table 6.1: Species data

6.1 Test on the Maxwell-Stefan model

The Maxwell-Stefan model can be derived from sytem (3.13) assuming the electrostatic potential as a given function. So it is possible to neglect the Poisson equation obtaining system (6.2).

Model 2 (Maxwell-Stefan)
Let Ω be a bounded domain of $\mathbb{R}^d$, d=1,2,3, $Q_T = \Omega \times (0,T)$, and $S_T = \partial\Omega \times (0,T)$, $T > 0$, the Maxwell-Stefan *model is given by*

$$
\begin{cases}
c_t \dfrac{\partial x_i}{\partial t} + \nabla \cdot \boldsymbol{N}_i = 0 & \text{in } Q_T \qquad (6.2a)\\
\displaystyle\sum_{\substack{j=1\\ j\neq i}}^{n} \frac{x_j \boldsymbol{N}_i - x_i \boldsymbol{N}_j}{c_t \text{Đ}_{ij}} + \sum_{\substack{j=1\\ j\neq i}}^{n} \frac{x_i x_j \left(\alpha_i - \alpha_j\right)}{\text{Đ}_{ij}} \frac{\nabla T}{T} & \\
\qquad = -\nabla x_i - \dfrac{x_i}{RT} z_{i,eff} \mathcal{F}\ \nabla\varphi & \text{in } Q_T \qquad (6.2b)\\
z_{i,eff} = \left(z_i - \omega_i \displaystyle\sum_{j=1}^{n} \frac{z_j x_j}{x_i} \right) & \qquad (6.2c)\\
\displaystyle\sum_{i=1}^{n} x_i = 1 & \qquad (6.2d)\\
\displaystyle\sum_{i=1}^{n} \boldsymbol{N}_i = 0 & \qquad (6.2e)\\
c_i(\boldsymbol{x}, 0) = \bar{c}_i(\boldsymbol{x}) & \text{in } \Omega \qquad (6.2f)\\
\boldsymbol{N}_i \cdot \nu = 0 & \text{on } S_T \qquad (6.2g)
\end{cases}
$$

for every $i = 1, \ldots, n-1$.

In the following sections we carry out the analysis of the Maxwell-Stefan model considering initially the effect of diffusion and subsequently including the contributions of temperature and electrical potential.

The one-dimensional mesh and temporal discretization are carried out in all the tests in this section with the data in Table 6.2.

ξ_0	$\Delta\xi$	ξ_{N_ξ}	t_0	Δ_t	t_{N_t}
0	0.001	1	0	0.01	0.2

Table 6.2: Mesh and temporal discretization data

6.1.1 The Maxwell-Stefan model: diffusion

We begin the analysis of the Maxwell-Stefan model (6.2) setting the temperature at $T = 300K$ and the electric potential equal to a constant. System (6.2) becomes:

$$\begin{cases} c_t \dfrac{\partial x_i}{\partial t} + \nabla N_i = 0 & \text{in } Q_T \quad (6.3a) \\ \displaystyle\sum_{\substack{j=1 \\ j\neq i}}^{3} \frac{x_j N_i - x_i N_j}{c_t Đ_{ij}} = -\nabla x_i & \text{in } Q_T \quad (6.3b) \\ \displaystyle\sum_{i=1}^{3} x_i = 1 & \text{in } Q_T \quad (6.3c) \\ \displaystyle\sum_{i=1}^{3} N_i = 0 & \text{in } Q_T \quad (6.3d) \\ c_i(\boldsymbol{x}, 0) = \bar{c}_i(\boldsymbol{x}) & \text{in } \Omega \quad (6.3e) \\ N_i \cdot \nu = 0 & \text{on } S_T \quad (6.3f) \end{cases}$$

Below are the tests of (6.3) carried out with three different profiles of initial concentrations $c^0_{i=1,2,3}$.

Test 1: Constant molar concentrations

$c_{S_1}(\cdot, 0)$	$c_{S_2}(\cdot, 0)$	$c_{S_3}(\cdot, 0)$
$1e5\ mol/m^3$	$2e5\ mol/m^3$	$7e5\ mol/m^3$

Table 6.3: Test 1, concentrations c_i at time $t = 0$.

Starting from the constant initial concentrations of Table 6.3 we get the results displayed in Figure 6.1. It can be clearly seen that, with the exception of numerical noise, the molar concentrations c_i (left column) remain constant and equal to the initial data and the molar flows N_i (right column) are null. In particular, these results agree with the predictions of the Fick model.

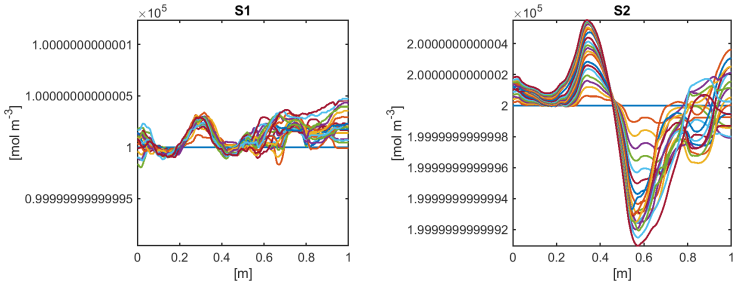

(a) c_{S_1}

(b) c_{S_2}

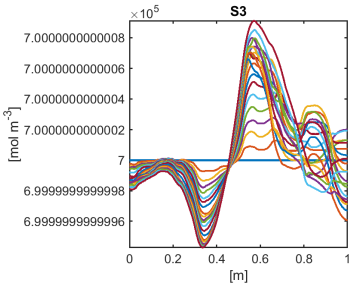

(c) c_{S_3}

Figure 6.1: Test 1: molar concentrations and molar fluxes

Test 2: Constant molar fractions

Repeating the previous test with the initial concentrations as in Figure 6.2 we get the results shown in Figure 6.3.

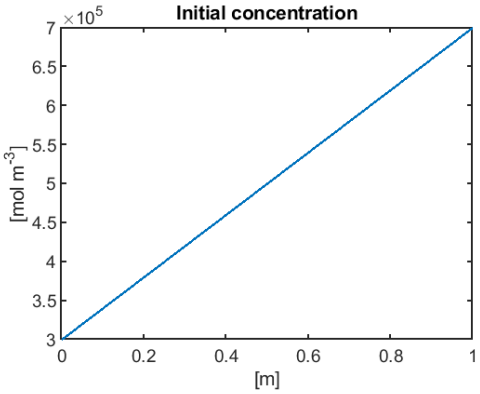

Figure 6.2: Test 2: molar concentrations c_i at time $t = 0$.

We immediately notice that the molar concentrations remain constant over time and equal to the initial data. These results may seem unexpected, but it should not be forgotten that both for the Maxwell-Stefan model and for the Fick model the driving force is generated by the gradient of the molar fraction and not by the gradient of the molar concentrations. Thus, in this test, although the latter are not null, the gradients of the molar fractions are zero. Let $c_S = c_{S_1}(\xi, 0) = c_{S_2}(\xi, 0) = c_{S_3}(\xi, 0)$ be the molar concentrations in Figure 6.2 of the three chemical species S_1, S_2 and S_3. We have that

$$x_i = \frac{c_i}{c_t} = \frac{C_S}{3 * C_S} = const \longrightarrow \nabla x_i = 0 \tag{6.4}$$

Then in the absence of driving forces the concentrations remain constant over time.

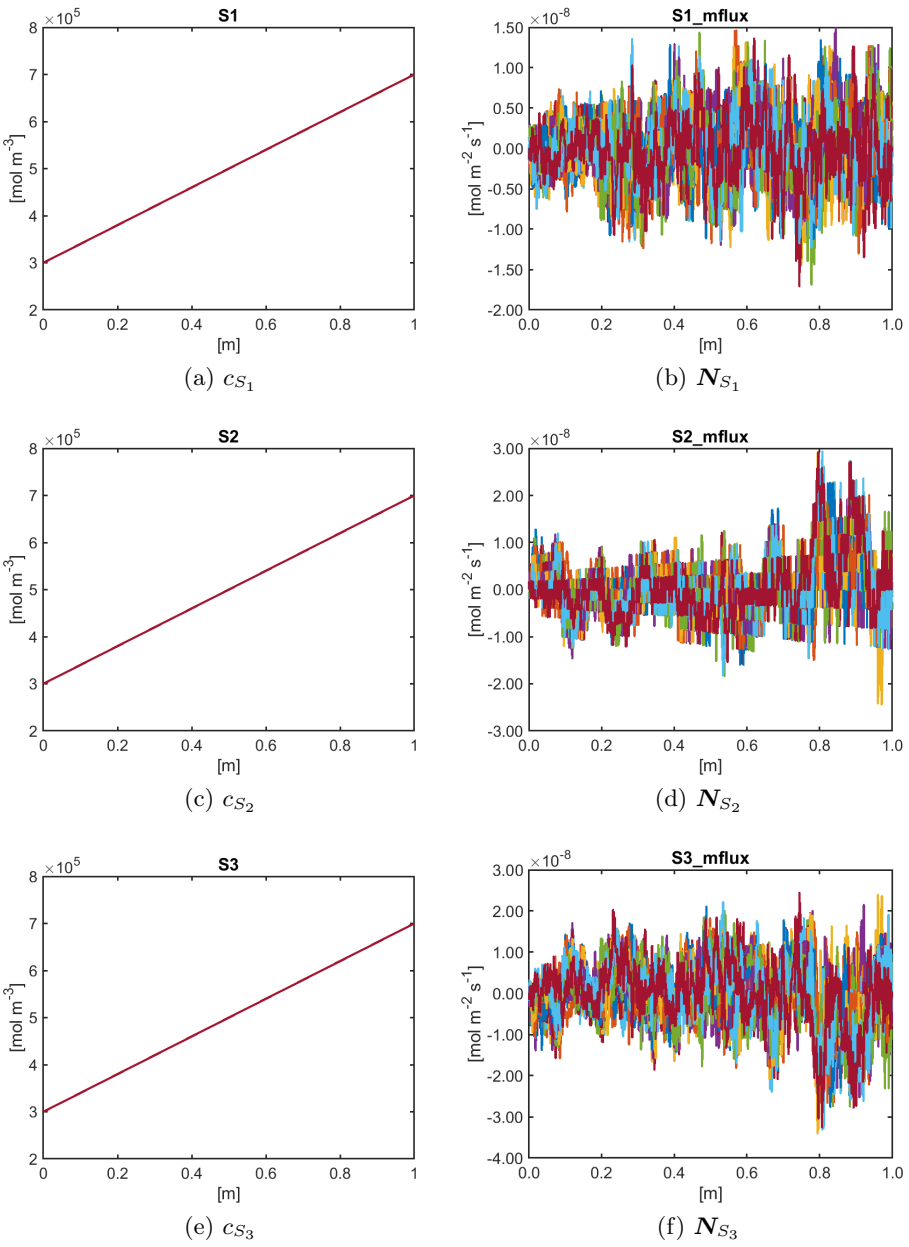

(a) c_{S_1} (b) $\boldsymbol{N}_{S_1}$

(c) c_{S_2} (d) $\boldsymbol{N}_{S_2}$

(e) c_{S_3} (f) $\boldsymbol{N}_{S_3}$

Figure 6.3: Test 2: molar concentrations and molar fluxes

Test 3: General molar concentrations

We consider the concentration profiles shown in Figure 6.2 as the initial data for molar concentrations c_i.

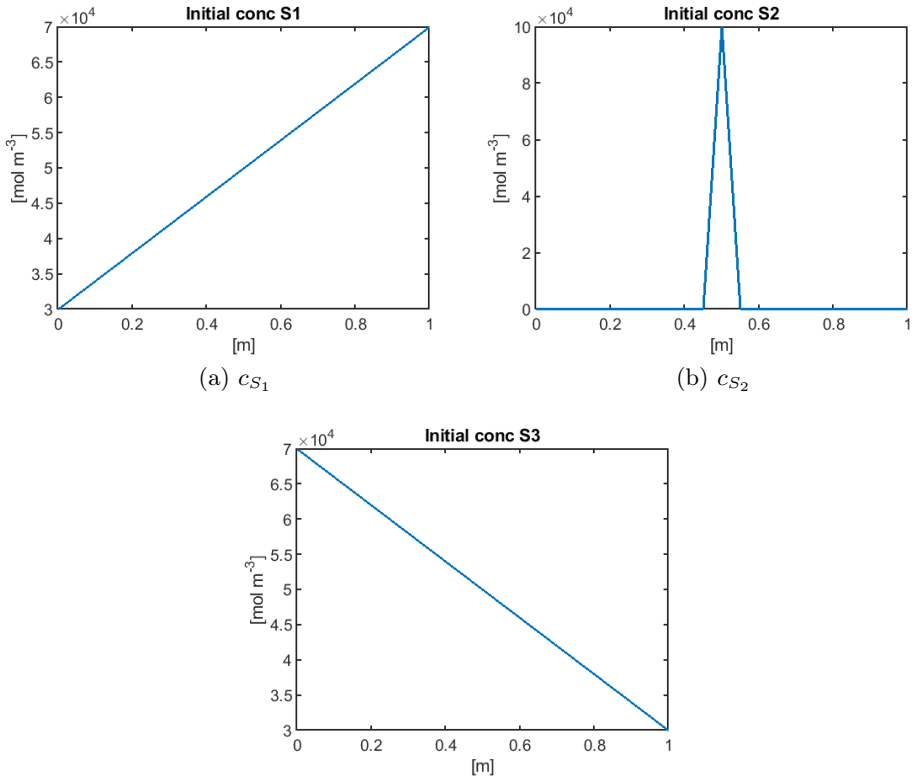

(a) c_{S_1} (b) c_{S_2}

(c) c_{S_3}

Figure 6.4: Test 3: initial molar concentrations

In this test we can observe the implications of the equimolar assumption. In fact, while the species S_2 diffuses from the concentration peak, the other two species S_1 and S_3 have an inverse diffusion and form concentration peaks, which are higher as the first one goes down. This phenomenon is caused by the equimolarity assumption, which imposes locally null total flux. It follows that species S_1 and S_3 in order to balance the outgoing flux of species S_2 from the peak, must have incoming fluxes that form concentration peaks.

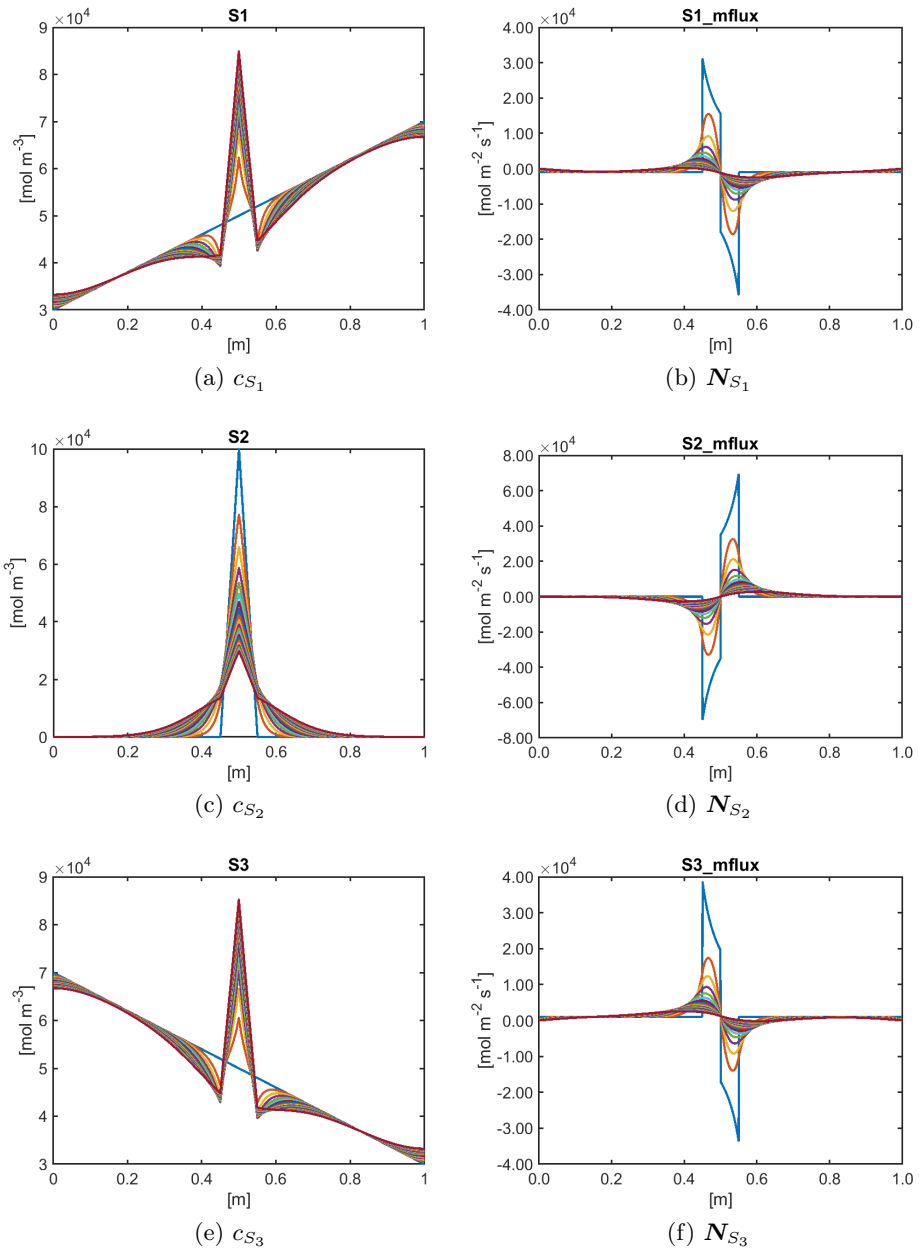

(a) c_{S_1} (b) $\boldsymbol{N}_{S_1}$

(c) c_{S_2} (d) $\boldsymbol{N}_{S_2}$

(e) c_{S_3} (f) $\boldsymbol{N}_{S_3}$

Figure 6.5: Test 3: molar concentration and molar fluxes

6.1.2 The Maxwell-Stefan model: diffusion and thermal gradient

We continue the analysis of the model (6.2) introducing a non-constant temperature profile. System (6.2) becomes:

$$\begin{cases} c_t \dfrac{\partial x_i}{\partial t} + \nabla N_i = 0 & \text{in } Q_T \quad (6.5a) \\ \displaystyle\sum_{\substack{j=1 \\ j\neq i}}^{3} \frac{x_j N_i - x_i N_j}{c_t \text{Đ}_{ij}} + \sum_{\substack{j=1 \\ j\neq i}}^{3} \frac{x_i x_j \left(\alpha_i - \alpha_j\right)}{\text{Đ}_{ij}} \frac{\nabla T}{T} = -\nabla x_i & \text{in } Q_T \quad (6.5b) \\ \displaystyle\sum_{i=1}^{3} x_i = 1 & \text{in } Q_T \quad (6.5c) \\ \displaystyle\sum_{i=1}^{3} N_i = 0 & \text{in } Q_T \quad (6.5d) \\ c_i(\xi, 0) = \bar{c}_i(\xi) & \text{in } \Omega \quad (6.5e) \\ N_i \cdot \nu = 0 & \text{on } S_T \quad (6.5f) \end{cases}$$

Test 4: Linear temperature profile

Test 4 is carried out with the initial constant concentrations c_i used in Test 1 (Table 6.3), the thermal diffusion coefficients in Table 6.4, multiplied by 10^5 to accentuate the effects of thermal diffusion, and the temperature distribution illustrated in Figure 6.6 .

$D^T_{S_1}$	$D^T_{S_2}$	$D^T_{S_3}$	
$0.31e-20$	$0.27e-20$	$1.95e-20$	$kg\ m^{-1}s^{-1}$

Table 6.4: Test 4, thermal diffusion coefficients

Observing the results in Figure 6.7 we notice that the chemical species S_2 moves in a direction consistent with the temperature gradient. Following a standard diffusion model we would expect a shift of the chemical species in the direction opposite to the temperature gradient. For convenience, let

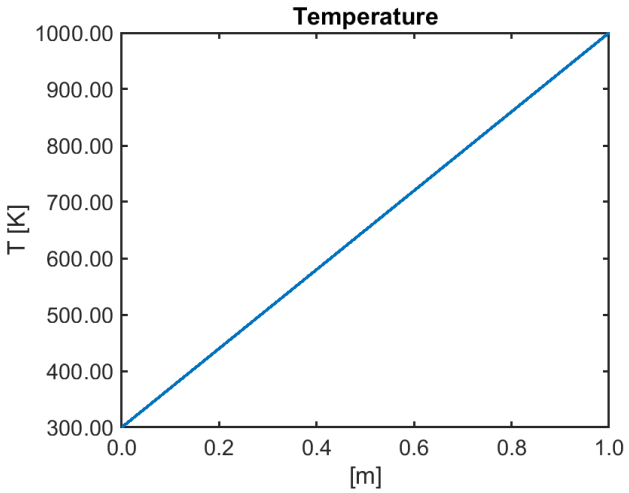

Figure 6.6: Test 4: linear temperature.

us define $\alpha_{i,eff}$ as follows:

$$\alpha_{i,eff} = \sum_{\substack{j=1 \\ j \neq i}}^{3} \frac{x_j \left(\alpha_i - \alpha_j\right)}{Đ_{ij}} = \sum_{\substack{j=1 \\ j \neq i}}^{3} \frac{x_j}{Đ_{ij}} \left(\frac{D_i^T}{\rho_i} - \frac{D_j^T}{\rho_j} \right) \tag{6.6}$$

$\alpha_{i,eff}$ is the weighted average of the thermal diffusivities differences $(\alpha_i - \alpha_j)$ multiplied by the inverse of the Maxwell-Stefan diffusion coefficients $Đ_{ij}$. Within the phenomenon of binary interactions among the species that is described by the equations of Maxwell-Stefan, $\alpha_{i,eff}$ is nothing but the thermal diffusivity that the species i exhibits averaging its diffusivity with the diffusivity of the species with which it interacts.

Let's try an easy example to understand the meaning of $\alpha_{i,eff}$. Suppose we have two different chemical species. Considered individually, if they are subjected to a temperature gradient, they move in the gradient opposite direction. Considered together, instead, these species interact, we could say that collide (see Section 2.3), and both try to go in the same direction. A "competition" is established between the species, only the faster species is able to move in the opposite direction to the temperature gradient, i.e. the one with the highest thermal diffusivity coefficient α_i. The other species is pushed in a direction consistent with the gradient. The difference $\alpha_i - \alpha_j$ is then divided by the Maxwell-Stefan diffusion coefficient $Đ_{ij}$, that weight

the obtained result on the interaction between the two species. If $Đ_{ij}$ is high then the interaction between species i and j is low. So it is not very advantageous to "win" on the other species. Since the Maxwell-Stefan model is based on binary interactions, in the case of multicomponent mixture a medium operation is required. Moreover we remember that the thermal diffusivity coefficients α_i are function of the mass density ρ_i, thus they change locally.

The $\alpha_{i,eff}$ in the Figure 6.7 can be ordered, for each point of the mesh, as follows:

$$\alpha_{S_2,eff} < 0 < \alpha_{S_3,eff} < \alpha_{S_1,eff}$$

Observing the corresponding molar concentrations we have that the species S_1, that has the greater $\alpha_{i,eff}$, moves in the opposite direction to the gradient by concentrating on the left boundary layer. Instead, species S_2, that has the lowest thermal diffusivity coefficient, moves and accumulates toward the right boundary layer. At the end, the species S_3, whose $\alpha_{i,eff}$ is positive and included between the other two, moves in the opposite direction to the thermal gradient. However, it has a concentration peak to the right of the left boundary layer, since the latter is occupied by the concentration peak of the species S_1.

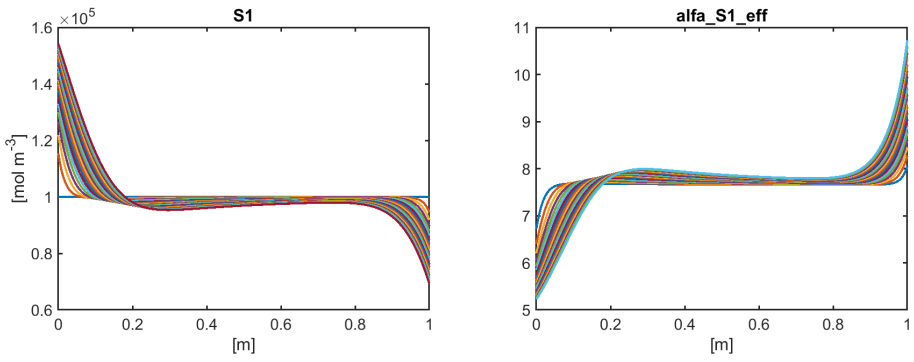

(a) c_{S_1}

(b) $\alpha_{S_1,eff}$

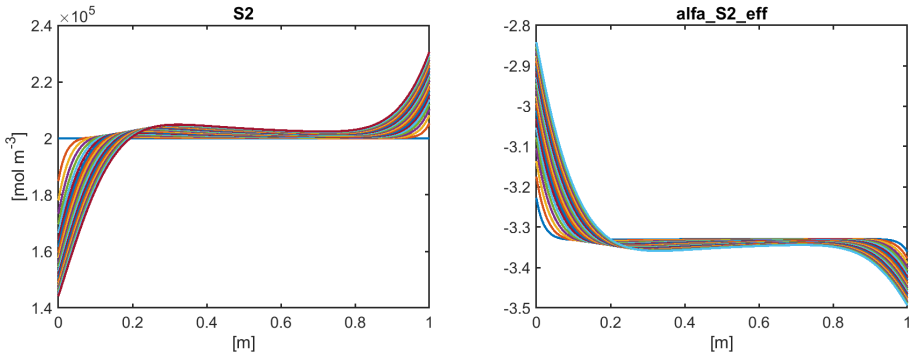

(c) c_{S_2}

(d) $\alpha_{S_2,eff}$

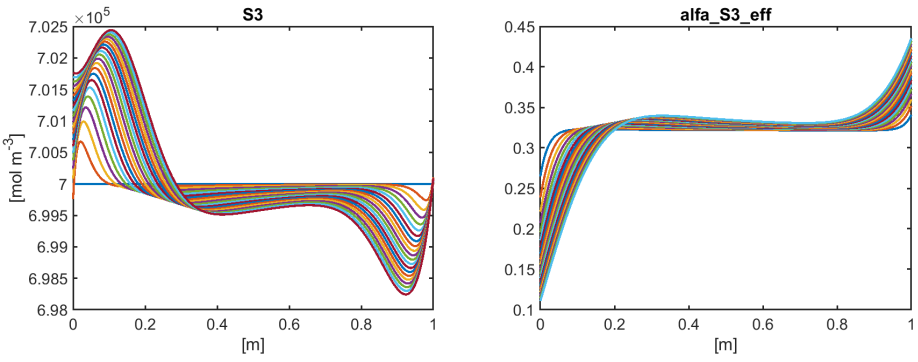

(e) c_{S_3}

(f) $\alpha_{S_3,eff}$

Figure 6.7: Test 4: molar concentrations and molar fluxes

6.1.3 The Maxwell-Stefan model: diffusion and electric potential

In this section we neglect the temperature effects by considering a constant temperature $T = 300K$ and we set a non-constant electric potential, as in Figure 6.8.

System (6.2) reads:

$$\begin{cases} c_t \dfrac{\partial x_i}{\partial t} + \nabla \cdot \boldsymbol{N}_i = 0 & \text{in } Q_T \quad (6.7a) \\ \displaystyle\sum_{\substack{j=1 \\ j \neq i}}^{3} \frac{x_j N_i - x_i N_j}{c_t \text{Đ}_{ij}} = -\nabla x_i - \frac{x_i}{RT} z_{i,eff} \mathcal{F} \nabla \varphi & \text{in } Q_T \quad (6.7b) \\ z_{i,eff} = \left(z_i - \omega_i \displaystyle\sum_{j=1}^{3} \frac{z_j x_j}{x_i} \right) & \text{in } Q_T \quad (6.7c) \\ \displaystyle\sum_{i=1}^{3} x_i = 1 & \text{in } Q_T \quad (6.7d) \\ \displaystyle\sum_{i=1}^{3} N_i = 0 & \text{in } Q_T \quad (6.7e) \\ c_i(\xi, 0) = \bar{c}_i(\xi) & \text{in } \Omega \quad (6.7f) \\ N_i \cdot \nu = 0 & \text{on } S_T \quad (6.7g) \end{cases}$$

Test 5: Linear electric potential

Given the initial constant concentrations c_i used in Table 6.5 and the ionic charges in Table 6.1, we get the results illustrated in Figure 6.9.

$c_{S_1}(\cdot, 0)$	$c_{S_2}(\cdot, 0)$	$c_{S_3}(\cdot, 0)$
2e5 mol/m^3	4e5 mol/m^3	4e5 mol/m^3

Table 6.5: Test 5, concentrations c_i at time $t = 0$.

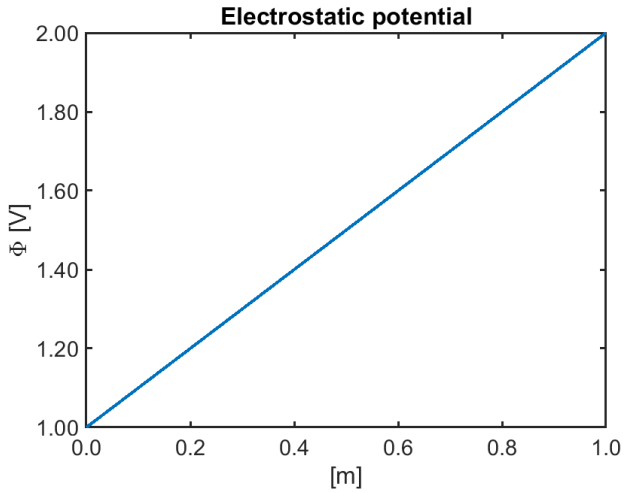

Figure 6.8: Test 5: electrostatic potential φ

Results in Figure 6.9 show that, despite the three ionic species are positive charged $z_i > 0$, they respond differently to the presence of the electric field (i.e the gradient of the electric potential). The positive ionic charge flows in the opposite direction to the electric potential gradient, however, the species $S2$ shows opposite behavior. This phenomenon is due to the interaction between the ionic species. The charge they are affected by is not the ion charge z_i but the effective charge $z_{i,eff}$. Considering the latter instead of z_i the concentration profiles obtained are easily understandable.

$$z_{i,eff} = z_i - \frac{M_i}{\sum_{j=1}^{n} x_j M_j} \sum_{j=1}^{n} z_j x_j$$

We can say that $z_{i,eff}$ is the actual charge of which a species is affected if it is subjected to interaction with other species. It is necessary to provide a physical interpretation of the effective charge $z_{i,eff}$. Mathematically it is defined as the difference between the ionic charge z_i and the average charge $(\sum_{j=1}^{n} z_j x_j)$ multiplied by the ratio between the molar weight M_i of the species i and the total molar weight of the mixture $\sum_{j=1}^{n} x_j M_j$.

Let us onsider the example of the previous Section 6.1.2. In this case the two species tend to move in the direction imposed by the gradient of the potential according with the sign of their charge. In the case of electroneutrality positive and negative charge are equal, so the charge flux (a current

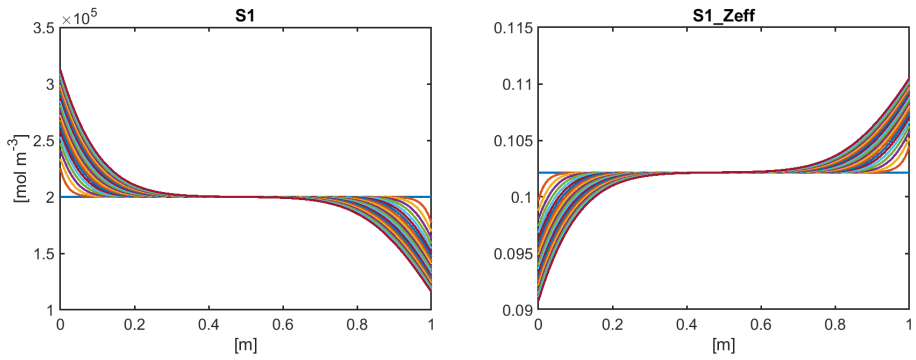

(a) c_{S_1}

(b) $Z_{S_1,eff}$

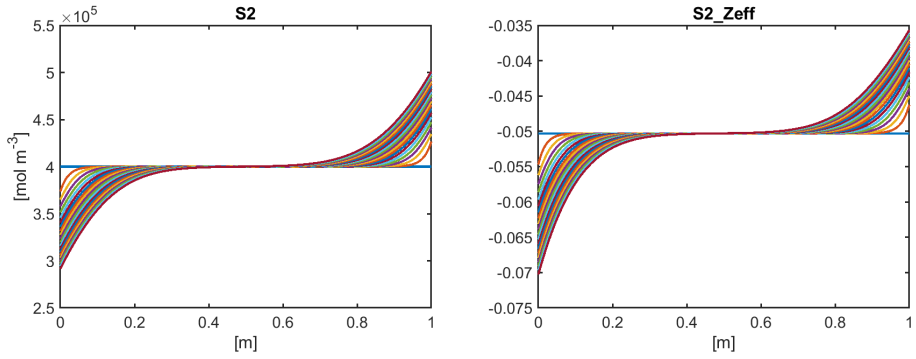

(c) c_{S_2}

(d) $Z_{S_2,eff}$

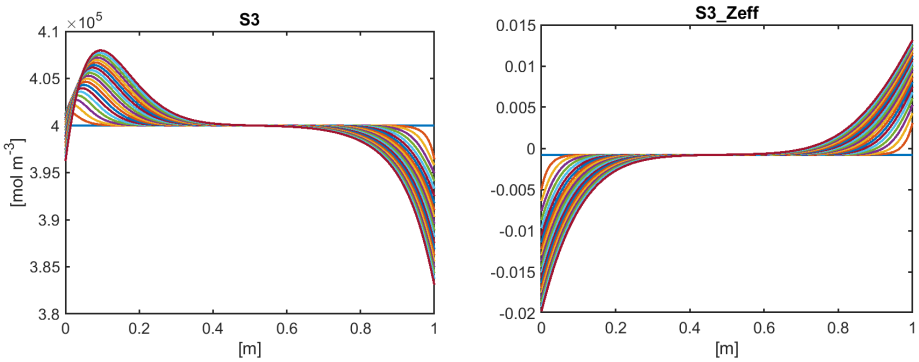

(e) c_{S_3}

(f) $Z_{S_3,eff}$

Figure 6.9: Test 5: molar concentrations and $z_{i,eff}$

density) that moves in one direction is equal and oppostite to that of the

other flux. Otherwise an excess of charge, we suppose positive charge, is formed. The accumulation of positive charges increases the interaction between the positive ionic species which decreases the effect of the potential on the positive ionic charge, in this case $|z_{i,eff}| < |z_i|$, whereas it increases the effect of the potential on the negative charged species $|z_{i,eff}| > |z_i|$. Since the average charge $\sum_{j=1}^{n} z_j x_j$ and total molar weight $\sum_{j=1}^{n} x_j M_j$ are equal for all $z_{i,eff}$, the molar weight of M_i is particularly relevant for the sign of $z_{i,eff}$.

6.2 Fick and Maxwell-Stefan models in the dilute mixture approximation

In this section we compare the Fick model and the Maxwell-Stefan model through the solutions provided by the two approaches for diluted and undiluted mixtures.

Model 3 (Fick's model)
Let Ω be a bounded domain of $\mathbb{R}^d$, d=1,2,3, $Q_T = \Omega \times (0,T)$, and $S_T = \partial\Omega \times (0,T)$, $T > 0$, the Poisson-Maxwell-Stefan *model is given by*

$$\begin{cases} \dfrac{\partial c_i}{\partial t} + \nabla \cdot \boldsymbol{N}_i = 0 & \text{in } Q_T \quad (6.8a) \\ \boldsymbol{N}_i = -D_i c_t \left(\nabla x_i + \dfrac{z_i q}{k_b T} x_i \nabla \varphi + \alpha_i x_i \dfrac{\nabla T}{T} \right) & \text{in } Q_T \quad (6.8b) \\ c_i(\boldsymbol{\xi}, 0) = \bar{c}_i(\boldsymbol{\xi}) & \text{in } \Omega \quad (6.8c) \\ \boldsymbol{N}_i \cdot \nu = 0 & \text{on } S_T \quad (6.8d) \end{cases}$$

for every $i = 1, \dots, n-1$.

Fick's model assumes that the mixtures are diluted. Mathematically, this condition is expressed as follows

$$c_i(\xi, t) \ll c_n(\xi, t) \qquad i = 1, \dots, n-1 \tag{6.9}$$

Equation (6.9) implies that

$$x_i = \frac{c_i(\xi,t)}{c_t(\xi,t)} \approxeq \frac{c_i(\xi,t)}{c_n(\xi,t)} \longrightarrow 0 \qquad i = 1, \dots, n-1 \tag{6.10a}$$

$$x_n = 1 - \sum_{i=1}^{n} x_i \longrightarrow 1 \tag{6.10b}$$

Let us impose conditions (6.10) on the $n-1$ Maxwell-Stefan relations (6.2b). System (6.2) becomes:

$$\begin{cases} c_t \dfrac{\partial x_i}{\partial t} + \nabla \cdot \boldsymbol{N}_i = 0 & \text{in } Q_T \quad (6.11a) \\ \boldsymbol{N}_i = -Đ_{in} c_t \left(\nabla x_i + \dfrac{x_i \alpha_i}{Đ_{in}} \dfrac{\nabla T}{T} + \dfrac{q\ z_{i,eff}}{k_b T} x_i \nabla \varphi \right) & \text{in } Q_T \quad (6.11b) \\ c_i(\boldsymbol{\xi}, 0) = \bar{c}_i(\boldsymbol{\xi}) & \text{in } \Omega \quad (6.11c) \\ \boldsymbol{N}_i \cdot \nu = 0 & \text{on } S_T \quad (6.11d) \end{cases}$$

In particular we have that:

$$x_i x_j \left(\alpha_i - \alpha_j\right) = x_i x_j \left(\frac{D_i^T}{\rho_i} - \frac{D_j^T}{\rho_j}\right)$$
$$= x_i x_j \left(\frac{D_i^T}{c_t x_i M_i} - \frac{D_j^T}{c_t x_j M_j}\right) = \frac{D_i^T x_j M_j - D_j^T x_i M_i}{c_t M_i M_j}$$

thus

$$\sum_{\substack{j=1 \\ j\neq i}}^{3} \frac{x_i x_j \left(\alpha_i - \alpha_j\right)}{Đ_{ij}} \frac{\nabla T}{T} = \sum_{\substack{j=1 \\ j\neq i}}^{3} \frac{1}{Đ_{ij}} \frac{D_i^T x_j \cancel{M_j} - \cancel{D_j^T x_i M_i}}{c_t M_i \cancel{M_j}} \frac{\nabla T}{T} \longrightarrow \frac{x_i}{Đ_{in}} \frac{D_i^T}{\rho_i} \frac{\nabla T}{T}$$

By equation (5.23) we get also

$$z_{i,eff} = z_i - \frac{M_i}{M_n} z_n$$

Let us define $\alpha_{i,Fick}$, $z_{i,Fick}$ and D_i as:

$$\alpha_{i,Fick} = \frac{\alpha_i}{Đ_{in}} \tag{6.12}$$
$$z_{i,Fick} = \left(z_i - \frac{M_i}{M_n} z_n\right) \tag{6.13}$$
$$D_i = Đ_{in} \tag{6.14}$$

Then, we obtain that, assuming diluted mixtures, the Maxwell-Stefan model (6.2) and the Fick model (6.8) are equivalent.

Relation (6.14) between the Maxwell-Stefan coefficients $Đ_{in}$ and the Fick diffusion coefficients D_i can be obtained by imposing conditions (6.10) into equation (2.41) and (2.39). Because the off-diagonal elements (2.39b) of the matrix $\boldsymbol{B}$ are all null

$$\boldsymbol{B} = \begin{bmatrix} \frac{1}{Đ_{1,n}} & 0 & \cdots & 0 \\ 0 & \ddots & & \vdots \\ \vdots & & \ddots & 0 \\ 0 & \cdots & 0 & \frac{1}{Đ_{n-1,n}} \end{bmatrix} \tag{6.15}$$

and the $\boldsymbol{\Gamma}$ matrix (2.17) is the identity matrix, by assumption of ideal mixture, the Fick diffusion coefficient matrix $\boldsymbol{D}$ is

$$\boldsymbol{D} = \begin{bmatrix} Đ_{1,n} & 0 & \cdots & 0 \\ 0 & \ddots & & \vdots \\ \vdots & & \ddots & 0 \\ 0 & \cdots & 0 & Đ_{n-1,n} \end{bmatrix} \tag{6.16}$$

that is the matrix version of the condition (6.14).

	$c_{S_1}(\cdot, 0)$	$c_{S_2}(\cdot, 0)$	$c_t(\cdot, 0)$
diluted	$1e2\ mol/m^3$	$2e2\ mol/m^3$	$1e6\ mol/m^3$
$\downarrow$	$1e4\ mol/m^3$	$2e4\ mol/m^3$	$1e6\ mol/m^3$
$\downarrow$	$1e5\ mol/m^3$	$2e5\ mol/m^3$	$1e6\ mol/m^3$
undiluted	$2e5\ mol/m^3$	$4e5\ mol/m^3$	$1e6\ mol/m^3$

Table 6.6: Initial concentration for Maxwell-Stefan and Fick comparison.

6.2.1 Maxwell-Stefan and Fick models: diffusion

In this section we compare the models (6.8) and (6.2) considering constant temperature $T = 300K$ and constant electric potential.

Let

$$c_i(\xi, t) = \frac{Q}{2\sqrt{\pi D_i t}} \exp\left(-\frac{\xi^2}{4D_i t}\right) \qquad i = 1, 2$$

where

$$Q = \int_{-\infty}^{+\infty} c_i(\xi, 0)\ d\xi$$

be the analytical solution of the problem (6.8) with initial condition, for $Q = 1$, $c_i^0 = \delta$ (where δ is *Dirac* delta) [19].

Computationally the initial molar concentrations c_i^0 are triangles of base length 0.002, centered in 0.5, and heights in Table 6.6. As can be seen from Figure 6.10, the two models are always equivalent whatever the height of the *Dirac* delta. This can be easily justified by the fact that delta concentrations are always diluted in a mixture composed with data in Table 6.6.

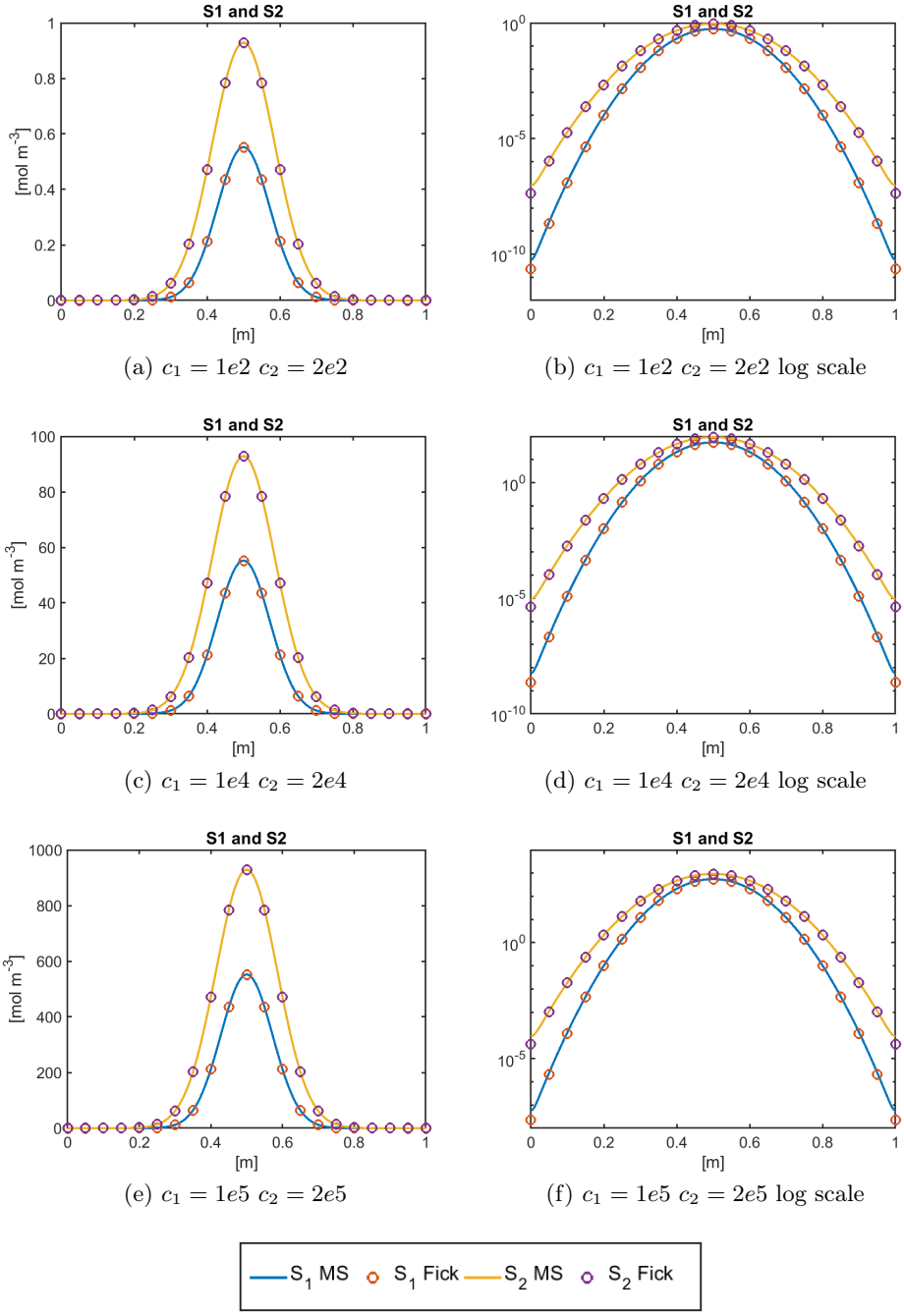

(a) $c_1 = 1e2$ $c_2 = 2e2$

(b) $c_1 = 1e2$ $c_2 = 2e2$ log scale

(c) $c_1 = 1e4$ $c_2 = 2e4$

(d) $c_1 = 1e4$ $c_2 = 2e4$ log scale

(e) $c_1 = 1e5$ $c_2 = 2e5$

(f) $c_1 = 1e5$ $c_2 = 2e5$ log scale

Figure 6.10: Comparison between Maxwell-Stefan and Fick models: the purely diffusive case

6.2.2 Maxwell-Stefan and Fick models: diffusion and thermal gradient

It is now assumed that the temperature $T = T(\xi)$ follows the linear profile shown in Figure 6.11 and that the electric potential is still constant.

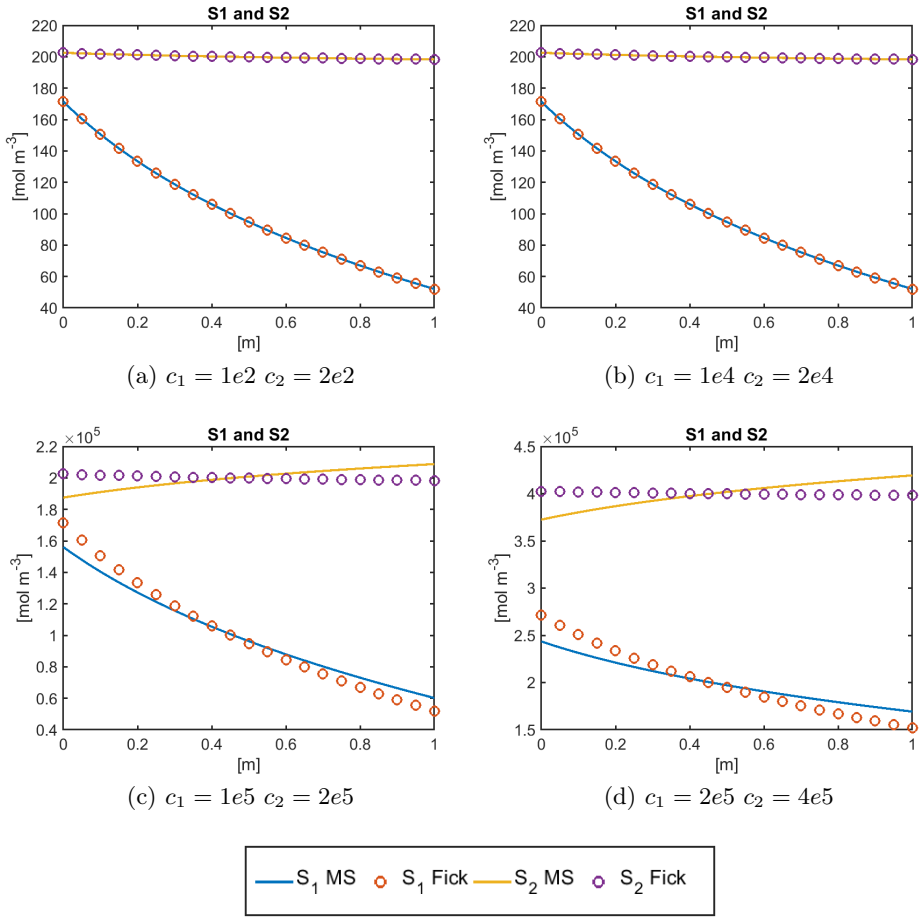

(a) $c_1 = 1e2$ $c_2 = 2e2$ (b) $c_1 = 1e4$ $c_2 = 2e4$

(c) $c_1 = 1e5$ $c_2 = 2e5$ (d) $c_1 = 2e5$ $c_2 = 4e5$

Figure 6.11: Comparison between Maxwell-Stefan and Fick models: linear temperature profile

Let

$$c_i(\xi) = -\alpha_{i,Fick} \ln(T(x)) + K \qquad i = 1, 2$$

where

$$K = \bar{c}_i + \frac{\alpha_{i,Fick}}{\xi_{N_\xi} - \xi_0} \left(\frac{T(\xi_{N_\xi})}{T'} \ln\left(T(\xi_{N_\xi})\right) - \frac{T(\xi_0)}{T'} \ln\left(T(\xi_0)\right) - \xi_{N_\xi} + \xi_0 \right)$$

$$\bar{c}_i = const$$

be an analytical solution of the steady state of the problem (6.8) ($\varphi = const$).

Graphs in Figure 6.11 show that, in the case of diluted mixtures, the Fick model of diffusion at the steady-state provides results that agree with the Maxwell-Stefan model, while, in the case of undiluted mixtures, the two models provide quite different results.

6.2.3 Maxwell-Stefan and Fick models: diffusion and electric potential

In this test we compare models (6.2) and (6.8) assuming a constant temperature profile $T = 300K$ and a linear electric potential function, as in Figure 6.8. Under these assumptions, equation (6.8b) is called *Nernst-Planck* equation.

Let

$$\varphi(\xi) = \varphi'\xi + \varphi(\xi_0)$$

be a potenzial profile with constant electric field. Then

$$c_i(\xi_0) = -\frac{c_i(\xi, 0)\,\lambda\left(\xi_{N_\xi} - \xi_0\right)}{e^{-\lambda\xi_{N_\xi}} - e^{-\lambda\xi_0}}\, e^{-\lambda\xi} \tag{6.17}$$

where

$$\lambda = \frac{z_{i,Fick}\; q\; \varphi'}{k_b T}$$

is a steady state solution of (6.8) for a constant temperature profile.

The comparison between the analytical steady-state solution (6.17) of the Fick model and the solution of the Maxwell-Stefan model, for t large enough, shows (see Figure 6.12) that in diluted mixture assumption the models are equivalent, whereas for undiluted mixure they produce different results.

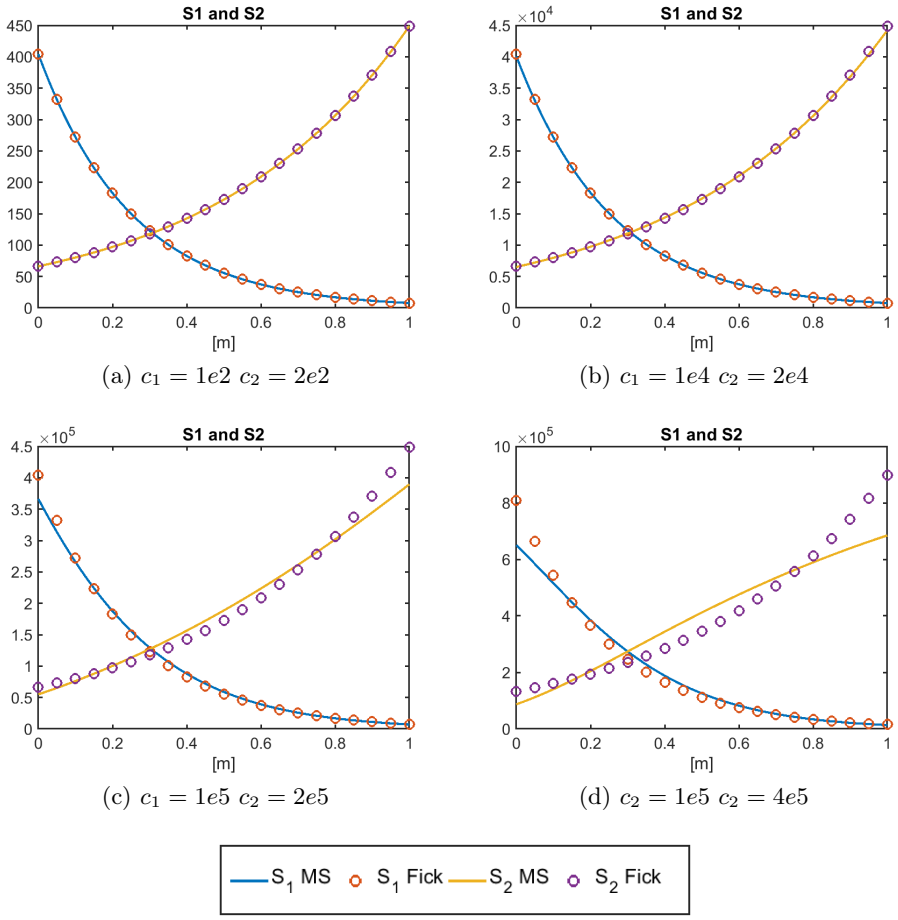

(a) $c_1 = 1e2$ $c_2 = 2e2$

(b) $c_1 = 1e4$ $c_2 = 2e4$

(c) $c_1 = 1e5$ $c_2 = 2e5$

(d) $c_2 = 1e5$ $c_2 = 4e5$

Figure 6.12: Comparison between Maxwell-Stefan and Fick models: constant electric field

6.3 Poisson-Nernst-Planck model

The aim of this section is to compare the Poisson-Maxwell-Stefan model (3.13) with the well-known Poisson-Nernst-Planck model. To this purpose let us introduce

Model 4 (Poisson-Nernst-Planck)
Let Ω be a bounded domain of $\mathbb{R}^d$, d=1,2,3, $Q_T = \Omega \times (0,T)$, and $S_T = \partial\Omega \times (0,T)$, $T > 0$, the Poisson-Nernst-Planck *model is given by*

$$\begin{cases} \dfrac{\partial c_i}{\partial t} + \nabla \cdot \boldsymbol{N}_i = 0 & \text{in } Q_T \qquad (6.18a) \\ \boldsymbol{N}_i = -c_t \mathrm{Đ}_{in} \left(\nabla x_i + \dfrac{\mathcal{F}}{R\,T} z_i x_i \nabla \varphi \right) & \text{in } Q_T \qquad (6.18b) \\ -\nabla \cdot (\varepsilon \nabla \varphi) = q \left(\displaystyle\sum_{i=1}^{n} z_i n_i + P \right) & \text{in } Q_T \qquad (6.18c) \\ c_i(\boldsymbol{x}, 0) = \bar{c}_i(\boldsymbol{x}) & \text{in } \Omega \qquad (6.18d) \\ \varphi = \bar{\varphi}_d & \text{on } S_T \qquad (6.18e) \\ \boldsymbol{N}_i \cdot \nu = 0 & \text{on } S_T \qquad (6.18f) \end{cases}$$

for every $i = 1, \ldots, n-1$.

Equation (6.18b) is the so called *Nernst-Planck* equation, that is the equivalent of equation (6.8b) for a costant temperature function. Combining the Nernst-Planck equation (6.18b) with continuity equation (6.18a) we get a conservation of mass equation that describes the motion of a diluted charged chemical species in a medium. It can be seen as an extention of the Fick's law of diffusion (2.6) for charged species that are moved by the presence of a non-constant electric potential, governed by the Poisson equation (6.18c). Moreover, we assume that the electroneutrality condition (3.5) holds only at the boundary where the electric potential is imposed.

Following the same procedure that it is used in Section 6.2 we can verify that, by defining $z_{i,NP}$ as in (6.13), the Nernst-Planck equation (6.18b) is only a limiting case of the generalized Maxwell-Stefan equation (3.13).

We are interested in a comparison between the Poisson-Maxwell-Stefan model (3.13) and the Poisson-Nernst-Planck model (6.18) starting by diluted mixtures up to undiluted mixtures. to this purpose we carry out the tests using the data in Tables 6.2, 6.1 and 6.6.

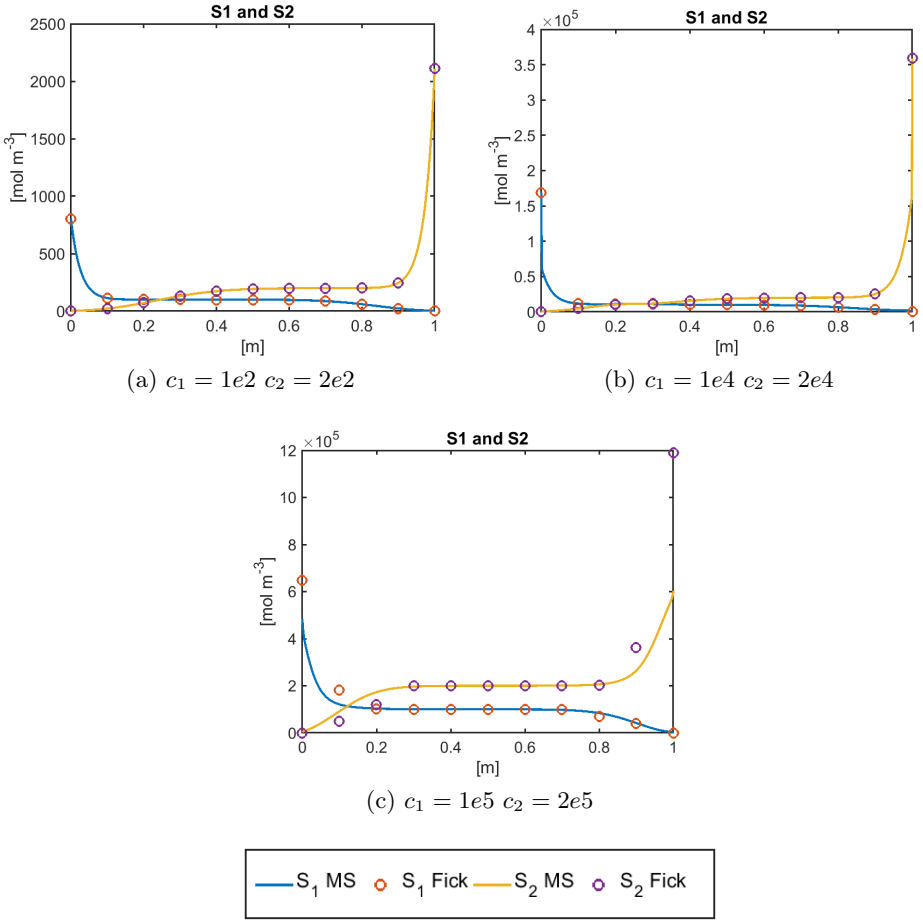

(a) $c_1 = 1e2$ $c_2 = 2e2$

(b) $c_1 = 1e4$ $c_2 = 2e4$

(c) $c_1 = 1e5$ $c_2 = 2e5$

Figure 6.13: Comparison between Poisson-Maxwell-Stefan and Poisson-Nernst-Planck models

Imposing an electric potential difference of 1 V at the boundary, Poisson-Maxwell-Stefan model and Poisson-Nernst-Plack model provide the results shown in Figure 6.13 Comparing these results we notice that in diluted mixture assumption the models are equivalent, whereas for undiluted mixure they produce quite different results.

Conclusions and future perspectives

In this work we focused on the Poisson-Maxwell-Stefan model with the aim of providing a detailed model for the description of mass transport. This model, discretized with the Galerkin Finite Element Method, is a system of nonlinear and coupled equations, therefore it requires a massive use of iterative algorithms for the decoupling and the solution of the linearized equations. In particular, the nonlinear Poisson equation is solved by Newton's method, whereas the system of continuity and Maxwell-Stefan equations exploits the potential of the Gummel Map. This resolutive framework has been implemented both for the Poisson-Maxwell-Stefan coupled problem and for the Maxwell-Stefan problem only, in the one-dimensional case using the Matlab programming language. In order to guarantee the existence and the uniqueness of the solution, a careful analysis of each step of the iterative process was carried out.

This code was tested with similar models and validated in the case of diluted mixtures, e.g. Fick's model of diffusion or Poisson-Nernst-Planck, providing good results. In particular, in contrast to the models mentioned above, the Posson-Maxwell-Stefan holds also for undiluted mixtures.

In conclusion we mention some possible directions for future works:

- extension of the code to 2D or 3D;
- implementation of non-standard stabilization techniques;
- include the dependence of the coefficients from physical quantities of the system;
- complete the integration with other physical forces;

- add the heat equation to the model;
- use c++ to speed up solution time.

Summary of physical relevant quantities

Name	Description	unit of measure
c_i	molar density of species i	$[mol\ m^{-3}]$
c_t	total molar density	$[mol\ m^{-3}]$
$\mathcal{F}$	Faraday constant	$[C\ mol^{-1}]$
$\boldsymbol{F}_i$	a general body force	$[N\ mol^{-1}]$
$\boldsymbol{J}_i$	relative molar flux of species i	$[mol\ m^{-2}s^{-1}]$
M_i	molar mass of species i	$[kg\ mol^{-1}]$
N_A	Avogadro constant	$[mol^{-1}]$
$\boldsymbol{N}_i$	molar flux of species i	$[mol\ m^{-2}s^{-1}]$
$\boldsymbol{N}_t$	total molar flux	$[mol\ m^{-2}s^{-1}]$
n	number of species in the mixture	$[-]$
n_i	number density of species i	$[m^{-3}]$
n_t	total number density	$[m^{-3}]$
p_i	partial pressure of species i	$[N\ m^{-2}]$
P	total pressure	$[N\ m^{-2}]$
q	electron charge	$[C]$
T	temperature	$[K]$
$\boldsymbol{u}_i$	velocity of species i	$[m\ s^{-1}]$
$\boldsymbol{u}$	average velocity	$[m\ s^{-1}]$
x_i	molar fraction of species i	$[-]$
z_i	charge number of species i	$[-]$
ε	dielectric constant	$[F\ m^{-1}]$
μ_i	molar chemical potential of species i	$[J\ mol^{-1}]$
ρ_i	species i density	$[kg\ m^{-3}]$
ρ_t	total density	$[kg\ m^{-3}]$
φ	electric potential	$[V]$
ω_i	density fraction of species i	$[-]$

Bibliography

[1] D. Bothe, "On the Maxwell-Stefan approach to multicomponent diffusion.", "Progress in Nonlinear Differential Equations and their Applications", *Springer*, pp. 81-93, 2011.

[2] L. Boudin, B. Grec, F. Salvarani, "A mathematical and numerical analysis of the Maxwell-Stefan diffusion equations", *Discrete and Continuous Dynamical Systems - B*, Vol. 17, No. 5, pp. 1427-1440, 2012.

[3] J. B. Duncan, H. L. Toor, "An experimental study of three component gas diffusion.", *A.I.Ch.E Journal*, Vol. 8, No. 1, pp. 38-41, 1962.

[4] V. Giovangigli, "Multicomponent Flow Modeling". *Birkhäuser*, 1999.

[5] H. K. Gummel, "A self-consistent iterative scheme for one-dimensional steady state transistor calculations". *Electron Devices*, pages 455-465, 1964.

[6] J. O. Hirschfelder, C. F. Curtiss, R. B. Bird, "Molecular Theory of Gases and Liquids". *Wiley, New York*, 1964.

[7] H. Hutridurga, F. Salvarani, "Existence and uniqueness analysis of a non-isothermal cross-fiffusion system of Maxwell-Stefan type.", *Applied Mathematics Letters*, Vol.45, pp. 108-113, 2018.

[8] J. D. Jackson, "Classical electrodynamics", *Wiley, New York*, 1999.

[9] J. W. Jerome, "Analysis of Charge Transport", *Springer*, 1996.

[10] A. Jüngel, I. V. Stelzer, "Existence analysis of Maxwell-Stefan system for multicomponent mixtures.", *SIAM Journal on Mathematical Analysis*, Vol.45, 2012.

[11] R. Krishna, R. Taylor "Multicomponent Mass Transfer", *Wiley*, 1993.

[12] R. Krishna, J. A. Wesselingh, "The Maxwell-Stefan approach to mass transfer.", *Chemical Engineering Science*, Vol. 52, No. 6, pp. 861-911, 1997.

[13] J. C. Maxwell, "On the dynamical theory of gases.", *Phil. Trans. R. Soc*, 157, pp. 49-88, 1866.

[14] S. Micheletti, A. Quarteroni, R. Sacco, "Current-Voltage Characteristics Simulation of Semiconductor Devices using Domain Decomposition", *J. Comp. Phys.*, 119, pp. 46-61, 1995.

[15] G. Novielli, A. Ghetti, E. Varesi, A. Mauri, R. Sacco, "Atomic Migration i Phase Charge Materials", *IEEE International Electron Devices Meeting* , 2013.

[16] R. D. Present, "Kinetic Theory of Gases", *McGraw-Hill*, 1958.

[17] J. M. Ortega and W. C. Rheinboldt, "Iterative Solution of Nonlinear Equations in Several Variables", *Academic Press,*, 1970.

[18] A. Quarteroni, "Numerical models for differential problems", *Springer-Verlag*, 2016.

[19] S. Salsa, "Partial Differential Equation in Action: From Modelling to Theory", *Springer*, 2016.

[20] J. Stefan, "Über das Gleichgewicth und die Bewegung insbesondere die Diffusion von Gasgemengen.", *Akad. Wiss. Wien*, 63, pp. 63-124, 1871.

[21] H. L. Toor, "Solution of the Linearized Equations of Multicomponent Mass Transfer: 1.", *A.I.Ch.E Journal*, Vol. 10, No. 4, pp. 448-455, 1964.

[22] H. L. Toor, "Diffusion in three component gas mixtures.", *A.I.Ch.E Journal*, Vol. 3, No. 2, pp. 198-207, 1957.